

INVESTIGATING AMINO ACID ACTIVATION OF G PROTEIN COUPLED
RECEPTORS INVOLVED IN LIPID METABOLISM

BY

MADELAINE D. RUSSELL

A thesis submitted to the
Department of Chemistry and Biochemistry
Mount Allison University
in partial fulfillment of the requirements for the
Bachelor of Science degree with Honours
April 22, 2020

ABSTRACT Energy homeostasis is a dynamic and complex process that maintains a balance between energy intake and expenditure. G protein coupled receptors (GPCRs), the largest family of transmembrane receptors, are critical for the cellular communication needed to coordinate processes involved in energy homeostasis (e.g. food intake). Indeed, metabolites are thought to act as sensors of energy stores by activating GPCRs in order to regulate energy homeostasis. Amino acids in particular have been shown to activate a growing number of GPCRs such as the calcium receptor (CaR), the orphan GPCRs GPR142 and GPR139, the purinergic receptor P2Y, and the hydroxycarboxylic acid receptor HCA3. This study aimed to further elucidate the role of monomeric amino acids as signaling molecules by employing a high throughput screen approach in which 19 monomeric amino acids were screened against 72 lipid metabolism GPCRs in a human cell line. Receptor activity was measured using the G-protein independent β -arrestin recruitment PRESTO TANGO assay. It was found that a mixture of 19 essential and non-essential amino acids significantly activated 14 lipid metabolism GPCRs. Of these, MC4, DP2, GPBA, S1P1, and S1P4 were chosen for further investigation and were found to be significantly activated by 0.8 mM *L*-Phenylalanine. This finding suggests *L*-Phenylalanine may play a more prominent role as a signalling molecule at GPCRs regulating energy homeostasis than previously thought. This aids in elucidating the satiating mechanisms of high protein diets and has important implications for research into diseases such as obesity, type 2 diabetes, and the metabolic syndrome.

ACKNOWLEDGMENTS

I would like to thank my supervisor Dr. Jillian Rourke for her continued support, guidance and expertise throughout this project and for cultivating my interest in metabolism. I would also like to thank my second reader, Dr. Vett Lloyd, for supporting my journey and growth as a scientist, and to my fellow lab mates Nick Fernandez, Brandon MacKinnon, Rachel McDougall, and Madeline Power for their collaboration in lab. I would also like to thank the honours seminar professor Dr. Jeffery Waller for improving my ability to convey scientific information. Special thanks goes to Mount Allison University, NSERC, NBIF, and NBHRF for supporting this research project. Finally, I would like to thank my family who gave me the opportunity to attend and fully immerse myself at Mount Allison University, to my friend Victoria who kept me thriving, and to Luke who always listened, kept me sane, and gave me strength.

Table of Contents

INTRODUCTION	4
G Protein Coupled Receptors	4
Metabolic GPCRs	6
Lipid Metabolism GPCRs	6
<i>GPCRs with Lipid Ligands</i>	7
<i>GPCRs with Non-Lipid Ligands that Alter Lipid Metabolism</i>	9
Amino Acids.....	14
<i>Amino Acid Metabolism and Transport</i>	14
<i>Intracellular Amino Acid Signaling</i>	16
<i>Amino Acid Signaling at GPCRs</i>	17
Rationale for the Current Study.....	19
MATERIAL AND METHODS	20
HTLA Cell Culture	20
DNA Preparation	20
Amino Acid Treatments	23
<i>Amino Acid Mixture for the High-Throughput Screen</i>	23
<i>Essential and Non-Essential Amino Acid Mixtures</i>	24
<i>Individual Amino Acid Treatment</i>	24
Presto Tango Assay	24
<i>Plating</i>	24
<i>Transfection</i>	25
<i>Treatment and Lysis</i>	25
<i>Luciferase and β-gal Assays</i>	26
Data Transformation and Statistical Analysis	27
<i>High-Throughput Screen Experiment</i>	28
<i>Non-Essential vs. Essential Amino Acid Mixture Experiment</i>	29
<i>Individual Amino Acid Experiment</i>	29
RESULTS	30
The High-Throughput Screen Reveals 6 Receptor Candidates as Amino Acid Sensors	30
<i>L-Phenylalanine</i> activates MC4, DP2, GPBA, S1P1, and S1P4	34
DISCUSSION	40
REFERENCES	55
APPENDIX	60

INTRODUCTION

Energy homeostasis is a dynamic and complex process that maintains a balance between energy intake and expenditure¹. This involves regulating an array of interlinked processes such as appetite, digestion, substrate use and storage, and biosynthesis¹⁻³. Evidently, there must be a mechanism for cells of various tissues and organs to communicate the energy status of the body in order to allow for coordinated responses such as insulin release, adipogenesis and lipolysis. These responses must be able to feed back to allow for amplification and/or inhibition and must be integrated and dynamically fine-tuned. Metabolites, such as sugars, fats, and proteins, play a crucial role in this crosstalk by activating membrane expressed G protein coupled receptors (GPCRs)⁴. This study aims to deepen the understanding of metabolite signaling at GPCRs by investigating amino acid activation of GPCRs involved in lipid metabolism. This study will act as the first step to further elucidate the coordination of amino acid metabolism and lipid metabolism, adipocyte function, appetite regulation, and other processes involved in energy homeostasis.

G Protein Coupled Receptors

GPCRs, the largest family of membrane spanning receptors, are critical for cellular communication^{5,6}. GPCRs are composed of seven transmembrane α -helices (TM) with alternating intracellular and extracellular loops, an extracellular amino terminus and an intracellular carboxyl terminus^{5,6}. They transmit extracellular signals into the cell by adopting a continuum of conformations upon agonist binding that allow them to couple to heterotrimeric GTPases (G protein)^{5,6}. Importantly, different ligands will stabilize a wide array of receptor conformations that differ in their coupling to effectors⁵.

Endogenous full agonists activate receptors by binding to the receptor's orthosteric site⁷. Competitive antagonists and inverse agonists compete for binding at the orthosteric site in order to maintain and decrease receptor constitutive activity, respectively⁷. Conversely, when a ligand binds to a GPCR at a site away from the orthosteric site, it is said to bind allosterically⁷. These ligands are referred to as allosteric agonists if they trigger receptor activation in the absence of the endogenous ligand⁷. This differs from allosteric modulators that alter the binding efficiency and/or signaling of an orthosteric ligand⁷. Importantly, some receptors, termed orphan receptors, currently have no known endogenous ligands⁸.

When activated, GPCRs act as guanine nucleotide exchange factors (GEFs) – meaning they trigger GDP release from the α -subunit of multiple heterotrimeric G proteins^{6,9}. The α -subunit conformation change, upon GTP binding, triggers dissociation from the $\beta\gamma$ -dimer and allows both to modulate multiple downstream effectors⁶. There are four main subclasses of $G\alpha$ proteins: stimulatory G proteins (G_s), inhibitory G proteins (G_i), G_q proteins, and G_{12} proteins. G_s and G_i activate and inhibit adenylyl cyclases (AC), respectively⁶. G_q proteins activate phospholipase C (PLC) that generates IP3 and DAG which increases Ca^{2+} influx and protein kinase C activity⁶. Finally, G_{12} activates RhoA GEFs that allow cytoskeleton reorganization⁶. The amplifiable nature of GPCR signaling requires the signal be rapidly shut off⁶. This is achieved by G protein coupled receptor kinases (GRKs) phosphorylating the carboxyl terminus serine and threonine residues in order to recruit arrestin^{6,10}. Arrestin sterically inhibits G protein coupling while also acting as an adaptor for clathrin and adaptin mediated internalization which results in either receptor recycling or degradation^{6,10}.

Metabolic GPCRs

GPCRs that bind to metabolites have recently been termed metabolic GPCRs⁴. Indeed, metabolites are now understood as signaling molecules that maintain energy homeostasis⁴. For example, hydroxycarboxylic acid (HCA) receptors bind to lactic acid (HCA1), various ketones (i.e. 3-hydroxybutyric acid; HCA2), and 3-hydroxyoctanoic acid (HCA3), a derivative of β -oxidation¹¹. Since these receptors are highly expressed in adipose tissue, metabolite signaling plays a crucial role in regulating lipolysis¹¹. More specifically, HCA1 signaling mediates lactate induced inhibition of lipolysis in adipose tissue either *via* an insulin induced paracrine/autocrine mechanism or due to an increase in circulating lactate during intensive exercise¹¹. HCA2 and HCA3 function during periods of starvation to prevent the depletion of adipocyte fat stores by binding to ketone bodies or intermediates of β -oxidation, respectively, to inhibit lipolysis¹¹. Another example of metabolite signaling occurs at the free fatty acid (FFA) receptors. FFA4 modulates the FFA induced changes to cyclooxygenase-2 (COX-2) expression *via* β -arrestin signaling to modulate adipocyte differentiation, hepatic and adipocyte lipogenesis, and insulin signaling³. These are only a few examples of an increasingly rich body of literature (Reviewed by Husted et al. (2017)) demonstrating the critical role of metabolite signaling at GPCRs.

Lipid Metabolism GPCRs

Similar to the functional grouping of metabolic GPCRs, this study will investigate metabolite signaling at a group of GPCRs involved in lipid metabolism. This group is composed of 72 Class A GPCRs that fall under two categories: receptors with known or putative lipid ligands and receptors that do not bind to lipid ligands, but whose activity

alters energy homeostasis (e.g. adipocyte function, energy intake). Below is a general discussion of the 72 lipid metabolism GPCRs with an emphasis on their link to lipid metabolism and/or energy homeostasis.

GPCRs with Lipid Ligands

The first category describes receptors that bind to lipids, a class of ubiquitous molecules that are characterised by the presence of hydrophobic moieties, but are highly structurally, chemically and functionally diverse^{12,13}. There are two main lipid biosynthetic pathways: carbanion condensation of acyl carrier protein intermediates, and the carbocation condensation of isoprene units¹². The former generates fatty acyl chains while the latter generates molecules such as prenols, sterols, aracheal glycerolipids, and shingolipids¹². Fahy *et al.* (2005) described a lipid classification system, based on the functional backbone of lipids, that generated 8 categories. Fatty acyls, for example, include fatty acids, octadecanoids, and eicosanoids – the latter includes endocannabinoids and lipoxygenases such as leukotriene^{12,13}. The other categories include glycerolipids, glycerophospholipids, sphingolipids, sterol lipids (e.g. estrogen), prenol lipids, saccharolipids, and polyketides.

Many of these lipid molecules, termed intracellular lipid mediators, have important signaling roles within the body as they are endogenous ligands for an array of GPCRs^{14–16}. Indeed, GPCRs that bind to lipid mediators account for 60 of the 72 lipid metabolism GPCRs investigated in this study; many of which were included on the basis of the phylogenetic tree constructed by Im *et al.* (2013). The GPCRs in this category include the cannabinoid receptors, leukotriene receptors, oxoglutarate receptor, estrogen receptor, bile acid receptor, platelet activating factor (PAF) receptor, prostanoid receptors,

succinate receptor, FFA receptors, HCA receptors, lysophospholipid receptors and the class A orphan receptors with putative lipid ligands.

The class A orphan receptors with putative lipid ligands were included based on the efforts made by Yin *et al.* (2009), Im *et al.* (2013) and Morales *et al.* (2018) in describing lipid signaling at orphan GPCRs. The phylogenetic tree constructed by Im *et al.* (2013) included the constitutively active GPR3, GPR6 and GPR12 that have been described as sphingosine 1-phosphate and sphingosyl-phosphorylcholine (SPC) receptors¹⁶. Also worth noting is the family GPR18, GPR55 and GPR119 orphan GPCRs that have been identified as putative endocannabinoid receptors¹⁷, but have not officially been de-orphanized due to inconsistent findings (as in Yin *et al.* (2009)).

Lipid mediators that bind to and alter the activity of GPCRs are integral for cellular processes such as cell proliferation, apoptosis and migration, and when deregulated, often contribute to an array of diseases including inflammatory diseases, cancer, and the metabolic syndrome¹⁸. Intermediates of phospholipid metabolism, such as lysophosphatidic acids (LPA) and sphingosine-1-phosphates are excellent examples of the critical roles these lipid mediators play, as they regulate cell survival, proliferation, shape, and migration by activating the LPA receptors (LPAR1-6) and the S1P receptors (S1P1-5), respectively^{19,20}. Regarding their role in energy homeostasis specifically, LPA, for example, acts in an autocrine/paracrine mechanism in adipocytes to regulate adipogenesis²¹. As for S1P, the ubiquitous $G_{i/o}$ coupled S1P1 receptor induces proliferation *via* activation of MAPK, PLC and Rac/Rho pathways in tissues including adipocytes¹⁹. Indeed, many if not all of the lipid mediators play critical roles in energy homeostasis. For example, the lipid components of bile referred to as bile acids (e.g.

phosphatidylcholine) bind to the gallbladder epithelium expressed bile acid receptor (GPBA) that alters chloride secretion and the size of the bile acid pool which ultimately alters dietary lipid absorption²². The first category of lipid metabolism GPCRs are thus inherently involved in energy homeostasis as they bind to intermediates of lipid metabolism and often modulate physiological processes such as adipocyte metabolism^{3,21}, nutrient uptake²², and inter-organ cross talk^{3,11}.

GPCRs with Non-Lipid Ligands that Alter Lipid Metabolism

The second category of lipid metabolism GPCRs describes receptors that do not bind to lipid mediators, but whose activity alters lipid metabolism and/or systemic energy homeostasis. By including receptors critical to energy homeostasis that have non-lipid ligands, this study will be able to more comprehensively examine metabolite signaling at GPCRs involved in lipid metabolism. This category of receptors includes the chemerin receptors, the adrenoceptors, the MECA cluster of receptors, and receptors that alter food intake (i.e. ghrelin, CCK).

Chemerin Receptors

The adipokine chemerin binds to the $G_{i/o}$ coupled CMKLR1 and GPR1 receptors, and regulates adipogenesis and lipid metabolism^{23,24}. Adipose tissue, whose canonical role has been a storage site for non-esterified fatty acids (NEFAs) in the form of triacylglycerol (TAG), has been shown to play a critical role as an endocrine organ that secretes an array of signaling peptides termed adipokines^{25,26}. One function of said adipokines is to bind to receptors expressed on adipocytes in order to regulate their differentiation and metabolism²⁵. Accordingly, one function of chemerin is to act in a paracrine/autocrine mechanism to enhance white adipose tissue (WAT) adipogenesis by

inducing proliferation and differentiation of pre-adipocytes^{24,25}. Furthermore, chemerin signaling may regulate lipolysis as chemerin levels are positively correlated with circulating triglycerides^{24,27}.

Adrenergic Receptors

The discussion on adipose tissue biology is also important when considering the effect of adrenergic receptors in energy homeostasis and lipid metabolism. The adipose organ is composed of two tissue types: WAT and brown adipose tissue (BAT)²⁶. These tissues differ in that BAT has greater vascularization, greater sympathetic nervous system innervation, and uses TAG for non-shivering thermogenesis, whereas WAT provides TAG systemically²⁶. Nonetheless, lipolysis in both of these tissues is mediated by adrenergic receptors; β 1AR and β 2AR are expressed in preadipocytes and β 3AR is expressed in differentiated adipocytes²⁶. During periods of low energy stores, adrenergic receptors expressed on white and brown adipocytes are activated^{26,28}. In WAT, activation of β adrenergic receptors culminates in lipolysis, whereas the opposite effect is mediated by the α 2ARs which allows for a fine tuning of adipocyte lipolysis^{26,28}. Moreover, activation of α 2ARs triggers lysophosphatidic acid production in adipocytes which mediates the LPA induced paracrine/autocrine regulation of adipogenesis²¹. In BAT, cold temperature activates the sympathetic nervous system (SNS) which triggers increased carbohydrate and lipid uptake in BAT which are oxidized to generate heat using the BAT specific mitochondrial uncoupling protein 1 (UCP1)²⁶. The adrenergic system is thus crucial for energy homeostasis through its regulatory actions at brown and white adipocytes.

MECA Cluster of Receptors

The MECA cluster of GPCRs, composed of the melanocortin receptors, endothelial differentiation gene receptors (EDG: S1P receptors and LPA receptors), cannabinoid receptors, adenosine receptors and the GPR3, GPR6, GPR12 orphan subset, was first described by Fredriksson and Schio (2005) and further elucidated by Morales *et al.* (2018). The MECA cluster includes receptors with conserved motifs and structural features that bind to peptides and lipids^{16,29}. Below is a brief discussion of the non-lipid binding MECA receptors' roles in regulating energy homeostasis.

Adenosine Receptors

Adenosine acts as a signal for low energy stores such that binding at the adenosine receptors activates ATP generating processes while inhibiting ATP consuming processes³⁰. Indeed, adenosine binds to the G_i coupled A1 and A3 receptors as well as the G_s coupled A2A and A2B receptors that have alternating roles in mediating adipocyte lipolysis³¹. Although adenosine was thought to mainly inhibit lipolysis in BAT and WAT *via* A1³⁰, it has been found that adenosine activating A2A actually increases lipolysis in BAT³¹. Furthermore, adenosine receptors seem to be intricately involved in sleep regulation, an important aspect of energy homeostasis³². In general terms, during prolonged wakefulness, increased levels of adenosine in certain brain regions, mainly the basal forebrain, induces sleep *via* adenosine binding to A1 and A2A³². The adenosine receptors are thus involved in maintaining energy homeostasis through a variety of processes including adipocyte metabolism and sleep regulation.

Melanocortin Receptors

The melanocortin system, composed of five receptors (MC1-MC5), has a diverse array of physiological and cellular roles within the body including, but not limited to, adrenocortical steroidogenesis, erectile response, exocrine gland secretion, and energy homeostasis³³. As for their role in energy homeostasis, the central nervous system (CNS) expressed MC3 and MC4 appear to be the most important as they play a crucial role in integrating peripheral signals communicating energy availability^{1,34,35}. Indeed, acute factors that assess the energetic status of the body, such as ghrelin and CCK, as well as longer term factors such as leptin and insulin, converge onto the melanocortin system to communicate changes to energy homeostasis³⁴. Therefore, in order to understand how these peripheral signals function, one must understand the general mechanisms of the central melanocortin system. MC3 and MC4 are activated by derivatives of proopiomelanocortin (POMC) and melanocyte stimulating hormones (MSH) that are synthesized and secreted by POMC neurons of the arcuate nucleus and the nucleus of the solitary tract^{1,34,35}. Importantly, the orexigenic agouti-related protein (Agrp) is a melanocortin receptor antagonist and is coexpressed with neuropeptide Y (NPY) in Agrp/NPY neurons¹. The melanocortin system plays integral roles in modulating food intake and peripheral energy expenditure^{1,34}. More specifically, increasing the melanocortin tone decreases food intake and increases energy expenditure, while decreasing the melanocortin tone increases food intake and promotes fat storage *via* the SNS shifting substrate utilization from fat to glucose^{1,34,36}.

Ghrelin and CCK

The final group of receptors are the class A GPCRs that alter food intake – the ghrelin receptor and the cholecystokinin (CCK) receptors. Ghrelin and CCK are peptide hormones that have opposing effects on food intake and energy expenditure^{37,38}. Ghrelin is released during periods of fasting by the stomach (along with other tissues such as the pituitary, hypothalamus, and the small and large intestines) and binds to the hypothalamic G_q coupled growth hormone secretagogue receptor (GHS-R) expressed on the orexigenic Agrp/NPY neurons and the anorexigenic POMC neurons to initiate food intake and decrease energy expenditure^{2,37}. GHS-R signaling in Agrp/NPY neurons results in depolarization and increased expression of NPY and Agrp, while GHS-R hyperpolarizes POMC neurons^{35,37}. Ghrelin also plays a role in modulating peripheral energy homeostasis as plasma ghrelin inhibits lipolysis and induces lipogenesis and triglyceride uptake in WAT₂ which facilitates anabolic processes following food intake³⁷. CCK, on the other hand, is released by the jejunum and duodenum during digestion, and interacts with the G_q coupled receptors CCK1, expressed in the pancreas, gall bladder, vagus nerve and areas of the CNS involved in appetite, and CCK2, expressed in the cerebral cortex, hypothalamus, vagus nerve and the gastric mucosa³⁹. CCK signaling reduces gastric emptying by modulating gastric muscular activity, promotes bile acid release and mediates short term suppression of food intake^{34,38,39}. CCK1's effect on satiety appears to involve activation of MC4 as well as a decrease in NPY expression in the dorsal medial hypothalamus (DMH)^{34,38}. These peptide hormones are thus released in response to low nutrient stores (ghrelin) and high nutrient stores (CCK) to modulate peripheral and central processes in order to efficiently and appropriately regulate energy homeostasis.

Amino Acids

It is clear then that cells must communicate the body's energy status to maintain energy homeostasis, and that metabolite and hormone (e.g. chemerin, cholecystokinin, ghrelin) signaling is critical for this communication. The above discussion focused on the role of lipid and peptide molecules in modulating metabolism through binding and altering the activity of a multitude of GPCRs. However, many other metabolites, such as monomeric amino acids, play critical roles in signal transduction as local or systemic levels (i.e. plasma concentrations) are indicative of the body's metabolic state⁴. The focus of this review will now shift to amino acids and their role in cellular communication. Amino acid classification, metabolism, and transport will first be discussed, followed by amino acid signaling and homeostasis. Finally, the literature on amino acid activation of GPCRs will be briefly reviewed.

Amino Acid Metabolism and Transport

Amino acids are generally understood as the building blocks of proteins and sources of fuel⁴⁰. Indeed, there are 20 *L*-amino acids that are used to synthesize proteins, and all amino acids can be oxidized to generate carbon backbones used in the tricarboxylic acid (TCA) cycle or for gluconeogenesis⁴⁰. The 12 essential amino acids (cysteine, phenylalanine, tyrosine, isoleucine, leucine, valine, arginine, methionine, threonine, histidine, tryptophan, and lysine) cannot be synthesized in the body and thus must be taken from the diet, whereas non-essential amino acids can be synthesized in most cells by amino transferases⁴⁰.

Ingested proteins are broken down in the GI tract – in the stomach, pepsin releases aromatic amino acids and polypeptides which are then hydrolyzed to free amino

acids in the duodenum by various peptidases⁴¹. Amino acids are transported across epithelial cells of the intestine such that they are absorbed into the blood stream⁴⁰. This results in a temporary rise in plasma amino acid levels from the otherwise constant 2.5 mM levels^{40,42}. Amino acids must be transported through the circulatory system to various organs and tissues in a highly dynamic and regulated process that contributes to amino acid homeostasis^{40,42}. During periods of high nutrient stores, excess amino acids are converted to glucose in the liver⁴². The liver is also important for amino acid catabolism since the toxic amino acid oxidation by-product ammonia is converted to urea via the urea cycle in this organ^{40,42}. Ammonia is finally excreted in the kidneys, which also secretes serine and converts citrulline to arginine, and phenylalanine to tyrosine^{40,42,43}.

Unsurprisingly, the majority of amino acids are found in muscle as they are taken up during periods of high nutrient stores in order to synthesize proteins, and secreted for hepatic gluconeogenesis during periods of low nutrient status^{40,42,44}. Adipose tissue also plays important roles in amino acid metabolism, most notably for branch chain amino acids (BCAAs), those being leucine, isoleucine and valine, which will be discussed in more detail later on⁴⁵.

A critical aspect of amino acid transport is their movement across cell membranes through ~50 mechanistically distinct transporters that regulate the intracellular amino acid pool⁴⁰. Many amino acid transport systems will exchange cytosolic non-essential amino acids such as glycine, alanine and glutamine for essential amino acids such as BCAAs⁴⁰. Cationic amino acids can be transported into the cell via facilitated diffusion

down their electrochemical gradient^{40,46,47}. Anionic amino acids, however, may be transported into the cell along with three Na⁺ and one H⁺ in exchange for one K⁺⁴⁰.

Intracellular Amino Acid Signaling

Amino acids have now been established as intracellular signaling molecules; they bind to and alter the activity of enzymes, transporters, and tRNA to trigger intracellular signaling cascades⁴⁰. The most well-known intracellular amino acid sensor is the mTORC1 complex that regulates protein synthesis and autophagy thereby playing a major role in amino acid homeostasis⁴⁰. When amino acids are abundant, they will activate mTORC1 such that protein synthesis increases and autophagy decreases, whereas during amino acid starvation, mTORC1 is inactive such that autophagy allows generation of amino acids^{40,45}. Activation of mTORC1 by amino acids requires phosphorylation of the TSC2 subunit by AKT or ERK signaling pathways, thereby allowing for integration of many signals to allow for a coordinated regulation of intracellular amino acid levels^{40,48}.

The equivocal role of BCAAs in metabolic health relates to their role in regulating the activity of mTORC1⁴⁵. BCAAs may be beneficial for metabolic health as they can activate mTORC1 in order to upregulate energy consuming processes, but constant mTORC1 activation may lead to insulin resistance *via* inhibitory phosphorylation of downstream insulin signaling effectors such as IRS-1 and IRS-2⁴⁵. Alternatively, BCAAs may trigger the onset of type 2 diabetes through altered BCAA metabolism that results in a build-up of toxic intermediates that damage pancreatic β cells⁴⁵. Altered BCAA metabolism may result from a decreased expression of BCAA metabolism genes in adipocytes of obese individuals thereby resulting in increased

plasma levels^{45,49}. BCAAs do appear to be tightly linked to pancreatic β cell function, as leucine regulates insulin release by activating glutamate dehydrogenase (GDH) which contributes to the closure of KATP channels allowing the depolarization necessary for Ca^{2+} mediated insulin release⁴⁰. Leucine also appears to be important for appetite regulation by acting as a sensor of dietary protein in the mediobasal hypothalamus⁵⁰. Since levels of BCAAs vary with a diet's protein content, changing levels of leucine exerts the anorectic effects of high protein diets by activating mTORC1 and/or by decreasing AMPK signaling in the hypothalamus to ultimately increase satiating pathways in the brain⁵⁰.

Other than the mTORC1 complex, amino acids also signal at uncharged tRNAs and transporters in order to maintain amino acid homeostasis⁴⁰. The signaling role of amino acids at uncharged tRNAs is indirect as the latter bind to various effector proteins such as protein kinase GCN2 (general control non-derepressable 2 system) to ultimately decrease translation and increase amino acid biosynthesis and transport⁴⁰. Activation of GCN2 also comes into play when examining the effect of amino acid imbalance on food intake⁵⁰. Amino acid imbalance is sensed in the anterior piriform cortex (APC), where an increase in uncharged tRNA concentrations of a particular amino acid leads to activation of GCN2 that alters glutamatergic signaling and thus food selection^{40,50}. The above discussion expands the traditional roles of amino acids as sources of fuel and biosynthetic intermediates to include intracellular signalling mediators.

Amino Acid Signaling at GPCRs

Recently, the extracellular signalling activity of amino acids at various GPCRs has provided evidence that many GPCRs may sense amino acids⁴. These amino acid-

sensing GPCRs include, but are not limited to, the taste 1 receptors (TAS1R2/3)⁵¹ and taste 2 receptors⁵², the calcium receptor⁵³, GPR142⁵⁴, P2Y⁵³, and HCA3⁵⁵.

Free amino acids present in food play an important and complex role in taste perception by binding to two main families of GPCRs – Taste 1 receptors and Taste 2 receptors⁴¹. More specifically, amino acids binding at taste receptors contributes to sweet, bitter and umami sensations⁵². Umami taste results from glutamate binding to a heterodimer formed by TAS1R1 and TAS1R3, whereas sweet taste results mainly from glycine and *D*-Tryptophan binding to a heterodimer of TAS1R1 and TAS1R2⁵². Importantly, glutamate also binds to the metabotropic glutamate receptor to impart umami taste⁴¹. Bitter taste, on the other hand, results from the complex interaction of *D* and *L* enantiomers of the 20 amino acids interacting with hetero and homodimers of the large family of Taste 2 receptors⁵².

Many of the novel amino acid sensing GPCRs belong to the Family C GPCRs that are characterized by their large extracellular Venus fly trap domain that allows them to form dimers and bind to various amino acids⁴¹. For example, *L*-amino acids have been shown to allosterically modulate the extracellular Ca²⁺ receptor (CaR), that regulates Ca²⁺ homeostasis in the parathyroid glands and kidneys⁵³. This allows for the coordination of digestive hormone secretion and amino acid digestion^{53,56}. However, there have been recent findings of amino acid activation of family A GPCRs, the focus of this study, such as *D*-amino acid activation of neutrophil expressed HCA3⁵⁵ and BCAA allosteric activation of the P2Y receptor⁵³. The former may contribute to the coordination of amino acid and lipid metabolism, and immune system activation⁵⁵. Importantly, *D*-amino acids are structurally and chemically distinct from HCAs⁵⁵ raising the possibility that this

ligand exerts its effects allosterically. These findings suggest that many GPCRs may sense amino acids, potentially *via* allosteric binding sites, such that complex cellular processes can be coordinated with the body's energy status⁵³.

Rationale for the Current Study

As can be seen in the above discussion of metabolite signaling, energy homeostasis is dynamic and complex and requires integration of multiple signals. The aim of this study is to investigate amino acid signalling at GPCRs involved in lipid metabolism in order to further our understanding of amino acids as extracellular signalling molecules. More generally, it is hypothesized that amino acid abundance may act as a sensor of energy stores or altered amino acid metabolism by binding to and modulating lipid metabolism GPCR signaling.

This study will employ a high-throughput screening (HTS) approach in human cells^{57,58} to measure the activation of the 72 lipid metabolism GPCRs by a mixture of 19 *L*-amino acids (*L*-Glutamine was absent from the mixture). More specifically, the response (i.e. luciferase expression) of lipid metabolism GPCRs will be measured following exposure to amino acids, using the PRESTO TANGO assay (see Fig. 1)^{57,58}. This assay system uses GPCR and β -arrestin fusion proteins. The GPCR carboxyl terminus is fused to a protease cleavage site that is then fused to a tetracycline transactivator (tTA) for a stably transfected luciferase reporter gene; whereas β -arrestin is fused to the protease specific for the GPCR fused cleavage site⁵⁸. Upon recruitment of β -arrestin to the ligand activated GPCR, the β -arrestin fused protease cleaves and releases the tTA from the GPCR, allowing it to enter the nucleus and irreversibly increase

luciferase expression⁵⁸. The transient activation of GPCRs is thus stabilized and measured *via* luminescence.

By elucidating the degree of amino acid metabolite signaling at lipid metabolism GPCRs, this study will act as the first step to further understanding how complex metabolic processes, i.e. lipid and amino acid metabolism, are coordinated to allow energy homeostasis. Furthermore, since the lipid metabolism GPCRs play varying roles in modulating appetite, adipose tissue growth, insulin signaling, and cholesterol and triacylglycerol levels, they are implicated in, and potential therapeutic targets for, obesity, diabetes and the metabolic syndrome^{3,20,21,23,39}.

MATERIAL AND METHODS

HTLA Cell Culture

The human embryonic kidney (HEK293) derived cell line, HTLA, containing the stably transfected tetracycline transactivator (tTA) dependent luciferase reporter gene as well as the β -arrestin2-Tobacco etch virus (TEV) fusion gene^{57,58}, were used for all experiments. HTLA cells were kept in high glucose (4.5 g/L) Dulbecco's Modified Eagle Medium (DMEM; Corning,10-013-CV) with 10% fetal bovine serum (FBS; Wisent Bioproducts, 234K18), 0.1 mg/mL hygromycin B (Bioshop, 8G55969), and 2 mg/mL puromycin (Bioshop, PUR333.100). Cells were grown at 37°C and 5% CO₂, passaged at 70% confluency with split ratios between 1:10 and 1:20, and grown to reach 40-60% confluency prior to plating in the PRESTO TANGO assay.

DNA Preparation

Escherichia coli (strain DH5 α) were transfected with DNA of interest, which is explained below, and grown on LB agar with 100 μ g/mL AMP (Fisher BP1760-5) for 18-

24 hours at 37°C and subsequently grown in 5 mL LB agar broth (100 µg/mL AMP) for 18-24 hours, at 37°C and 250 rpm. DNA was extracted and purified using the NucleoSpin Plasmid Transfection-grade mini prep kit (Macherey-Nagel, 740490.250). Control DNA included pCMV- β -galactosidase (β -gal), lysophosphatidic acid receptor 1 (LPAR1) PRESTO TANGO plasmid (Kroeze *et al.*, 2015), and pBSK (empty vector). The 72 lipid metabolism PRESTO TANGO GPCRs (see Table 1) and the positive control PRESTO TANGO LPAR1 were obtained from the Barnea lab as outlined by Kroeze *et al.* (2015).

Table 1: The family, assigned receptor number, International Union of Basic Clinical Pharmacology (IUPHAR) nomenclature, names of the corresponding PRESTO TANGO plasmids, and class of the 72 lipid metabolism GPCRs analyzed in this study.

Family	Receptor numbers	IUPHAR names	PRESTO TANGO name	Class
Adenosine receptors	R1, R2, R3, R4	A1, A2A, A2B, A3	ADORA1, ADORA2A, ADORA2B, ADORA3	A
Cannabinoid receptors	R5, R6	CB1, CB2	CNR1, CNR2	A
G protein estrogen receptor	R7	GPGR	GPGR	A
GPR18, GPR55, GPR119	R8, R9, R36	GPR18, GPR55, GPR119	GPR18, GPR55, GPR119	A
Leukotriene receptors	R10, R11, R12, R13, R14, R15	BLT1, BLT2, CysLT1, CysLT2, OXER, FPR2	LTB4R, LTB4R2B, CYSLTR1, CYSLTR2, OXER1, FPR2	A
Melanocortin receptors	R16, R17, R18, R19, R20	MC1, MC2, MC3, MC4, MC5	MC1R, MC2R, MC3R, MC4R, MC5R	A
Oxaglutarate receptor	R21	OXGR1	OXGR1	A
Platelet activating factor receptor	R22	PAF	PTAFR	A
Prostanoid receptor	R23, R24, R25, R26, R27, R28, R29, R30, R31	EP3, FP, EP1, TP, EP4, EP2, IP, DP1, DP2	PTGER3, PTGFR, PTGER1, TBXA2R, PTGER4, PTGER2, PTGIR, PTGDR, GPR44	A
Succinate receptor	R32	SUCNR1	SUCNR1	A
Orphan class A	R33, R34, R35, R36, R37, R38, R39, R40	GPR65, GPR68, GPR174, GPR119, GPR34, GPR183, GPR3, GPR6	GPR65, GPR68, GPR174, GPR119, GPR34, GPR183, GPR3, GPR6	A
Bile acid receptor	R41	GPBA	GPBA	A
Chemerin receptors	R42, R43	Chemerin receptor 1, Chemerin receptor 2	CMKLR1, GPR1	A
CCK receptors	R44, R45	CCK1, CCK2	CCKAR, CCKBR	A
Free fatty acid receptors	R46, R47, R48, R49	FFA1, FFA2, FFA3, FFA4	FFA1, FFA2, FFA3, GPR120	A
Ghrelin receptor	R50	Ghrelin receptor	GHSR	A
HCA receptors	R51, R52, R53	HCA1, HCA2, HCA3	HCA1, HCA2, HCA3	A
Lysophospholipid receptors	R54, R55, R56, R57, R58, R59, R60, R61, R62, R63	LPA1, LPA2, LPA4, LPA5, LPA6, S1P1, S1P2, S1P3, S1P4, S1P5	LPAR1, LPAR2, LPAR4, LPAR5, LPAR6, S1PR1, S1PR2, S1PR3, S1PR4, S1PR5	A
Adrenoreceptors	R64, R65, R66, R67, R68, R69, R70, R71, R72	alpha1A, alpha1B, alpha1D, alpha2A, alpha2B, alpha2C, beta1, beta2, beta3	ADRA1A, ADRA1B, ADRA1D, ADRA2A, ADRA2B, ADRADC, ADRB1, ADRB2, ADRB3	A

Amino Acid Treatments

Amino Acid Mixture for the High-Throughput Screen

In the High-Throughput Screen (HTS), the lipid metabolism GPCRs were treated with a mixture of essential amino acids (minimal essential medium (MEM) Sigma Aldrich, M5550 50X) and non-essential amino acids (Wisent Bioproducts, MEM 321-011-EL) prepared in Opti-MEM (Gibco, 31985-070). The essential amino acids were diluted from the stock (50X) mixture to 4X such that cells were treated with (in mM) 2.9 *L*-Arg HCl, 1.0 *L*-Cys 2HCl, 1.0 *L*-His HCl H₂O, 1.6 *L*-Ile, 1.6 *L*-Leu, 2.0 *L*-Lys HCl, 0.4 *L*-Met, 0.8 *L*-Phe, 1.6 *L*-Thr, 0.2 *L*-Trp, 0.8 *L*-Tyr, and 1.6 *L*-Val. The non-essential amino acids were diluted from the stock mixture (100X) to 8X resulting in concentrations (mM) of 0.8 *L*-Ala, 0.9 *L*-Asn H₂O, 0.8 *L*-asp, 0.8 *L*-glu, 0.8 *L*-Gly, 0.8 *L*-Pro, and 0.8 *L*-Ser. These concentrations were based off of those used by Conigrave *et al.* (2000) which mimic fasting amino acid levels. The mixture of 4X essential amino acids and 8X non-essential amino acids prepared in Opti-MEM (pH 9) is referred to as 4/8X aa for simplicity. Toxicity of the 4/8X aa mixture was analyzed by a thiazoyl blue tetrazolium bromide (MTT) assay (see appendix Fig. 1). The MTT assay followed the same protocol as the PRESTO TANGO assay, however instead of lysis buffer, 20 μ L of 1 mg/mL MTT was added to each well and incubated for 2 hours at 37°C. Media was removed and 100 μ L of dimethyl sulfoxide (DMSO) was added to each well and incubated with shaking for 15 minutes to solubilize the formazan product. Absorbance was measured at 570 nm. The MTT assay revealed the 4/8X aa mixture significantly increased cell number (Appendix Fig. 1), which was corrected for by measuring β -galactosidase expression as described below.

Essential and Non-Essential Amino Acid Mixtures

Following the HTS, the 6 receptor candidates identified were treated with VEH, the 4/8X aa mixture, the 4X Essential amino acid mixture (E) alone, or the 8X Non-Essential amino acid mixture (NE) alone, in order to identify which mixture contained the amino acid of interest. The 4X Essential amino acid mixture and the 8X Non-Essential amino acid mixture were prepared as outlined above in Opti-MEM.

Individual Amino Acid Treatment

The 6 receptor candidates identified in the HTS were treated with the individual essential amino acid solutions that were prepared in MiliQ H₂O at concentrations (mM) of 36.3 *L*-Arg (Sigma A5006), 12.9 *L*-Cys 2HCl, 13.5 *L*-His HCl H₂O (Bioshop HIS200.25), 20.0 *L*-Ile, 20.0 *L*-Leu (Bioshop LEU222.25), 24.8 *L*-Lys HCl (Sigma C6001), 5.1 *L*-Met, 10.0 *L*-Phe (TCI P0134), 20.0 *L*-Thr (TCI T0230), 2.5 *L*-Trp (TCI T0541), 9.9 *L*-Tyr (Bioshop TYR333.25), and 20.0 *L*-Val (Bioshop VAL201.25). NaOH was used to dissolve *L*-His and *L*-Tyr, the latter was also heated at 37°C overnight and subsequently stored at 37°C. All other amino acids were stored at 4°C. Solutions were diluted in Opti-MEM such that cells were treated with the concentrations detailed in the 4X essential amino acid mixture. The pH of all 12X amino acid solutions were tested and fell within 7.97 and 9.17.

Presto Tango Assay

A summary of the PRESTO TANGO assay is shown in Figure 1.

Plating

On the day of plating, media was removed and cells were washed with serum free DMEM (Corning,10-013-CV). Cells were incubated for 2 minutes at room temperature

(RT) with 0.25% trypsin and 2.21 mM EDTA (Wisent Bioproducts, 325-043-EL). Cells were centrifuged in 5 mL of complete DMEM (Corning, 10-013-CV with 10% FBS) at 300x g for 5 min. The cell pellet was resuspended in serum free DMEM and diluted to 200,000 cells/mL and 5% FBS. 100 μ L of cells were plated at 10,000 cells/well, 5% FBS in a 96 well plate and incubated at 37°C and 5% CO₂ for 24 hours to allow for attachment.

Transfection

HTLA cells were transiently transfected with 50 ng/well pBSK, 25 ng/well pCMV- β -gal plasmid DNA and either 25 ng/well positive control LPAR1 DNA or 25 ng/well of one of the 72 lipid metabolism GPCRs using polyethylenimine (PEI; SigmaAldrich). Negative control cells for transfection were transiently transfected with 75 ng/well pBSK and 25 ng/well pCMV β -gal plasmid DNA. The transfection components outlined above were prepared in Opti-MEM and incubated with 0.02 mg/mL PEI for 15 minutes at RT and subsequently diluted 1 in 5 with Opti-MEM. 70 μ L of the 5% FBS DMEM was removed from the plated HTLA cells prior to addition of the transfection solution (50 μ L). The cells were incubated at 37°C and 5% CO₂ for 12-18 hours.

Treatment and Lysis

30 μ L of the cell's media was removed and replaced with 20 μ L of the amino acid treatment or vehicle (VEH; Opti-MEM). Each experiment was performed in three sets (A, B, C) which function as biological triplicates. Within each set, all treatments and controls were performed in technical triplicates. Each 96 well plate contained triplicate LPAR1 expressing HTLA cells treated with 10% FBS (prepared in Opti-MEM; n=81 in

HTS) and VEH (Opti-MEM, n=81 in HTS) that acted as the positive control for receptor activation. The pBSK negative transfection control cells were treated with Opti-MEM. Cells were incubated at 37°C and 5% CO₂ for 24 hours. All media was removed prior to the 15 min incubation with 20 µL of 1X Firefly lysis buffer (Biotium, Cat# 99923), lysis was completed by freezing cells at -80°C.

Luciferase and β -gal Assays

All steps of the following protocol were performed at RT. The cell lysate was thawed, diluted 1 in 10 with Milli-Q water and resuspended on a microplate shaker for 2 minutes. The β -gal assay was performed in a 96 well plate by incubating 30 µL of the cell lysate with 1X β -gal assay buffer (0.1 M sodium phosphate buffer (pH 7.3), 1 mM MgCl₂, 0.067% (w/v) ortho-nitrophenyl- β -galactosidase (ONPG), 50 mM β -mercaptoethanol) for 10 minutes prior to absorbance being read at 420 nm (A₄₂₀) in a SpectraMax M3 microplate spectrophotometer. A blank for the 1X Firefly lysis buffer was diluted and assayed in triplicate.

The luciferase assay was performed in a white 384 well plate (Greinerbio-one 781075) by incubating 20 µL of the 1 in 10 diluted cell lysate with 0.08 mg/mL *D*-luciferin (Biotium, 9907) in assay buffer (Biotium, 30028L) for 5 min with oscillation. Luminescence was measured as relative luminescence units (RLU) using the BioTek Synergy HT luminescence reader and Gen5 software. A lysis buffer blank was diluted and assayed in triplicate.

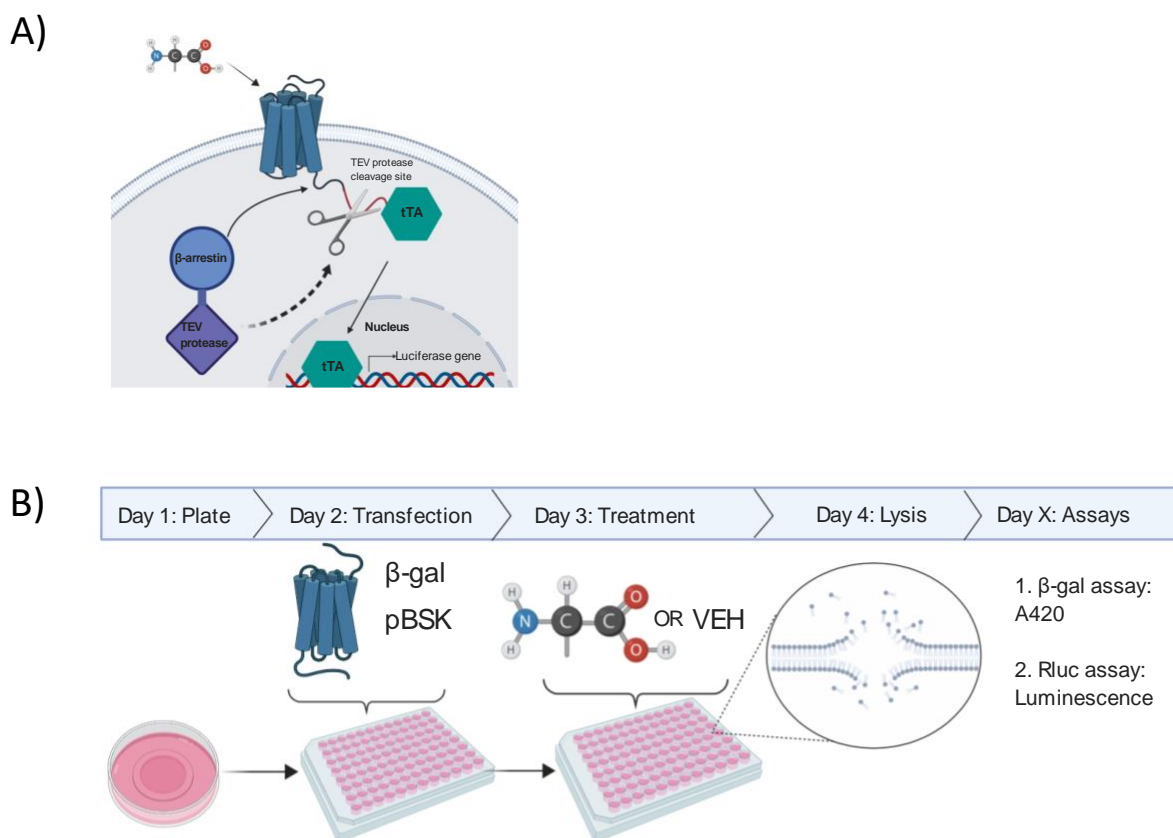


Figure 1: Experimental Time Line of the PRESTO TANGO Assay. Receptor activity was measured using the PRESTO TANGO assay^{57,58} **A)** Activated receptors recruit a β -arrestin-TEV protease fusion protein which brings the TEV protease close to its cleavage site and thus releases tTA. tTA travels to the nucleus and increases luciferase expression. Figure based on that of Kroeze *et al.* (2015). **B)** HTLA cells were plated at 25 000 cells/well and incubated for 24 hours after which they were transfected with pBSK (empty vector DNA), β -galactosidase DNA (pCMV-Bgal), and the PRESTO-Tango GPCR of interest using polyethylenimine (PEI). The next day, they were treated with the amino acid treatment condition or vehicle and incubated for 24 hours. The cells were then lysed and stored at -80°C . Receptor activity was quantified via a luciferase assay and β gal assay.

Data Transformation and Statistical Analysis

Each experiment was performed in biological triplicates referred to as Sets A, B and C. In each set, every experimental condition was measured in technical triplicates (LPAR1 activation was measured in 9 technical replicates in each set of the HTS). For all experiments, each well's RLU was divided by its average lysis buffer blank adjusted

A420 in order to account for potential differences in cell number and/or degree of receptor expression caused by different treatment conditions. The A420 adjusted RLU (RLU/A420) values for each treatment condition are represented as the average value across the three sets with the standard error of the mean. Average fold change was calculated by dividing each well's RLU/A420 by the average RLU/A420 of that receptor's VEH treatment, and are also represented with standard error of the mean.

All statistical analyses were performed with a significant *p*-value set at 0.05. Statistical analysis for the positive control LPAR1 data from each experiment was performed in Prism5. The non-parametric Mann-Whitney U test was used to measure significant differences between LPAR1 VEH RLU/A420 and LPAR1 10% FBS RLU/A420 combined from all three sets for each experiment, respectfully.

High-Throughput Screen Experiment

Statistical analysis for all of the HTS data were performed in R studio, with the exception of the positive control LPAR1 data being performed in Prism5. Statistical analyses were performed first on each set (A, B and C) separately and subsequently with all sets combined. The Shapiro test for normal distribution and Bartlett's test for homogeneity of variances were performed on each receptor's triplicate RLU/A420 VEH and 4/8X aa treatment condition(s). If both tests were passed, the parametric T-test was used to measure significant differences between VEH and 4/8X aa treatment condition for each receptor. If one of the tests failed, the non-parametric Mann-Whitney U test was used in the place of the T-test. Only receptors with significant differences when data from all three sets were combined were identified as receptor candidates and used for subsequent analysis.

Non-Essential vs. Essential Amino Acid Mixture Experiment

The RLU/A420 of each receptor's VEH, 4/8X, E, and NE treatment conditions were log₁₀ transformed and outliers were identified and removed using the boxplot function in R studio. The Shapiro test for normal distribution and Bartlett's test for homogeneity of variances were performed on the log₁₀ transformed data in R studio. Prism 5 was used to perform the parametric one-way ANOVA on each receptor with a Bonferroni post-hoc test to compare every pair of treatment conditions. Data is represented as boxplots of RLU/A420 showing mean, and highest and lowest values.

Individual Amino Acid Experiment

The RLU/A420 of each receptor's VEH, and individual essential amino acid treatment conditions were log₁₀ transformed and outliers were identified and removed using the boxplot function in R studio. The Shapiro test for normal distribution and Bartlett's test for homogeneity of variances were performed on the log₁₀ transformed data in R studio. Prism 5 was used to perform the parametric one-way ANOVA on each receptor with a Dunnett post-hoc test to compare each essential amino acid treatment condition to VEH. Due to unequal variances and/or failure to pass the assumption of normal distribution, Cys and Trp data from MC4, and Trp data from S1P4, were excluded from the respective parametric one-way ANOVAs. The non-parametric Kruskal-Wallis test with the Dunns post hoc test was used to compare MC4 Cys and Trp to MC4 VEH. The non-parametric Mann-Whitney U test was used to compare S1P4 Trp to S1P4 VEH. Data is represented as boxplots of RLU/A420 showing mean, and highest and lowest values.

RESULTS

The High-Throughput Screen Reveals 6 Receptor Candidates as Amino Acid Sensors

This study investigated metabolite signaling at GPCRs involved in lipid metabolism by employing a high-throughput screen methodology using the G-protein independent PRESTO-TANGO assay to measure receptor activation. HTLA cells were transfected with the positive control GPCR LPAR1, or 1 of 72 lipid metabolism GPCRs prior to treatment with 10% FBS, or a mixture of 19 *L*-amino acids, respectively. It is well established that serum contains soluble LPA, the agonist of LPAR1, at sufficient levels to trigger receptor activation⁵⁹. Indeed, across the three biological replicates, treatment with 10% FBS significantly increased RLU/A420 of LPAR1 expressing cells compared to VEH (Fig. 2A) with an average fold change of 17 ± 2 relative to VEH.

Compared to VEH, the 4/8X aa treatment resulted in significantly increased RLU/A420 for 13 lipid metabolism GPCRs (A1 (R1), BLT1 (R10), MC4 (R19), OXGR1 (R21), EP3 (R23), DP2 (R31), GPR6 (R40), GPBA (R41), GPR1 (R43), FFA1 (R46), FFA4 (R49), S1P1 (R59), S1P4 (R62)), and significantly decreased RLU/A420 of 1 lipid metabolism GPCR (CCK1 (R44)), when data from set A, B and C were combined for statistical analyses (Fig. 2B). Interestingly, by examining the VEH RLU/A420 of the 14 receptor candidates, one can note that they have drastically different constitutive activities (Fig. 2B). The average VEH RLU/A420 of A1, MC4, OXGR1, EP3, DP2, GPBA, CCK1, GPR1, and FFA4 fall within the range of 10,000 to 40,000, which is at least an order of magnitude greater than that of BLT1, and at least an order of magnitude less than those of GPR6, FFA1, S1P1, and S1P4.

Of the 14 receptor candidates, GPBA showed the greatest fold change in RLU/A420 of the 4/8X aa treatment compared to VEH with an average of 3.7 ± 0.3 (Fig. 2C). MC4, DP2, S1P1, and S1P4 all had very similar average fold changes relative to VEH across the three sets of 2.4 ± 0.3 , 2.4 ± 0.6 , 2.4 ± 0.7 , and 2.5 ± 0.3 , respectively. OXGR1 and FFA1 are the only other receptor candidates that have a fold change between 4/8X aa treatment and VEH of at least 2, those being 2.1 ± 0.4 , and 2.0 ± 0.1 , respectively. A1, BLT1, EP3, GPR6, GPR1, and FFA4 only showed fold changes within the range of 1.5 (BLT1 and GPR6) to 1.9 (A1). Since these receptors (A1, BLT1, EP3, GPR6, GPR1, and FFA4) had lower fold changes in RLU/A420 of the 4/8X aa mixture relative to VEH, they were excluded from further analysis, as this indicates lower biological significance. Unlike the other 13 receptor candidates, the 4/8X aa treatment resulted in a significant decrease in RLU/A420 for CCK1 expressing cells compared to VEH, corresponding to an average fold change of 0.50 ± 0.06 relative to VEH (Fig. 2B and C).

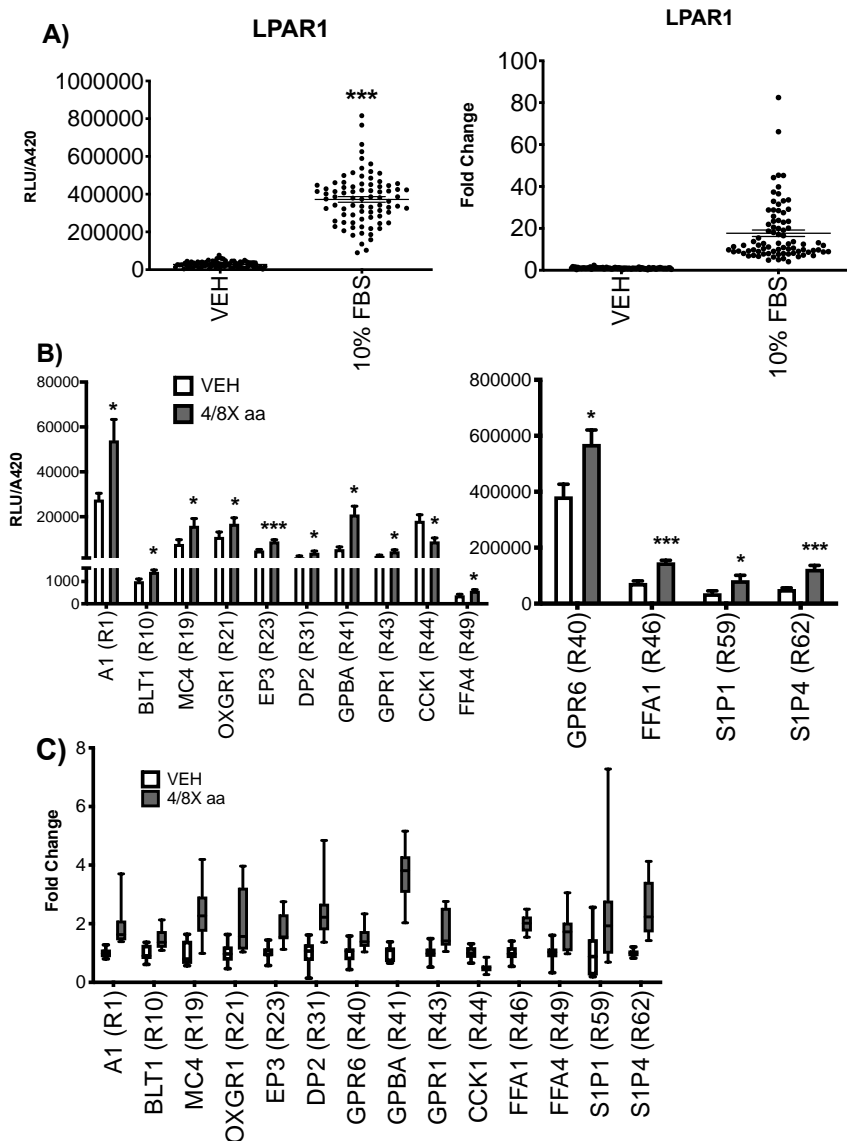


Figure 2: The Essential and Non-Essential Amino Acid Mixture Significantly Alters the Activities of 14 Lipid Metabolism GPCRs. Receptor activation was measured following a PRESTO-TANGO β -arrestin recruitment assay. HTLA cells were transiently transfected with GPCR PRESTO TANGO plasmids as indicated. **A)** The relative luminescence units (RLU) adjusted by β -galactosidase expression (absorbance at 420 nm; Left), and fold change RLU/A420 (Right) of the positive control lysophosphatidic acid 1 (LPAR1) PRESTO TANGO receptor treated with Opti-MEM vehicle (VEH) and 10% fetal bovine serum (FBS). **B)** The RLU/A420 of the 14 lipid metabolism GPCRs whose activities were significantly altered by treatment with the 4X essential 8X non-essential amino acid (4/8X aa; grey) mixture compared to Opti-MEM VEH (white) following the high-throughput screen of the 72 lipid metabolism GPCRs. Note the different range in RLU/A420 for the two sets of receptors. **C)** Fold change RLU for data from B. All box plots are shown as highest and lowest values; Bar plots are mean and SEM, and scatter plots represent individual data points showing mean and SEM. Statistical significance (*P < 0.05. ***P < 0.0001) was evaluated using a parametric T-test or the non-parametric Mann-Whitney U test (for R1, R41, R62, and LPAR1) using RLU/A420 data combined from three biological replicates performed with technical triplicates.

In order to more closely examine the effect of the 4/8X aa mixture on the activity of these 14 receptor candidates, and to compare them to the rest of the 72 lipid metabolism GPCRs, statistical analyses were performed on each biological replicate separately. Significance levels (*p*-values) resulting from these statistical evaluations are shown in a heat map ranging from white (*p* = 1.00) to dark blue (*p* = 0.00) (Fig. 3). This allows for visualization of the consistency with which the 4/8X aa mixture significantly activated the 14 receptor candidates. A1, MC4, EP3, DP2, GPBA, GPR1, CCK1, FFA1, and S1P4 appeared to be more consistently activated by the 4/8X aa mixture across the three replicates compared to BLT1, OXGR1, GPR6, FFA4, and S1P1. The significance levels in each set (A, B, and C) of the former group of receptors all fall within the range of *p*=0.002 to *p*=0.186 corresponding to the darker blue colours in each set. The latter group of receptors all have at least one lighter blue set that corresponds to significance values between *p*=0.365 to *p*=0.768. Also important to note, there appears to be a trend for many receptors to have significant *p*-values in at least one set. Indeed, GPR65 (R33), GPR68 (R34), GPR34 (R37), GPR183 (R38), CCK2 (R45), and LPA5 (R57) in set A, CysLT2 (R13), EP3 (R23), GPR3 (R39), CMKLR1 (R42), HCA2 (R52) and beta3 (R72) in set B, and finally OXER (R14), FPR2 (R15), GPR65 (R33), GPR3 (R39), CCK2 (R45), and FFA2 (R47) in set C had significant *p*-values when RLU/A420 of the 4/8X aa treatment was compared to VEH (Appendix Table 1). However, these receptors were not investigated any further due to the lack of significant changes in RLU/A420 when all sets were analyzed together (Appendix Table 1).

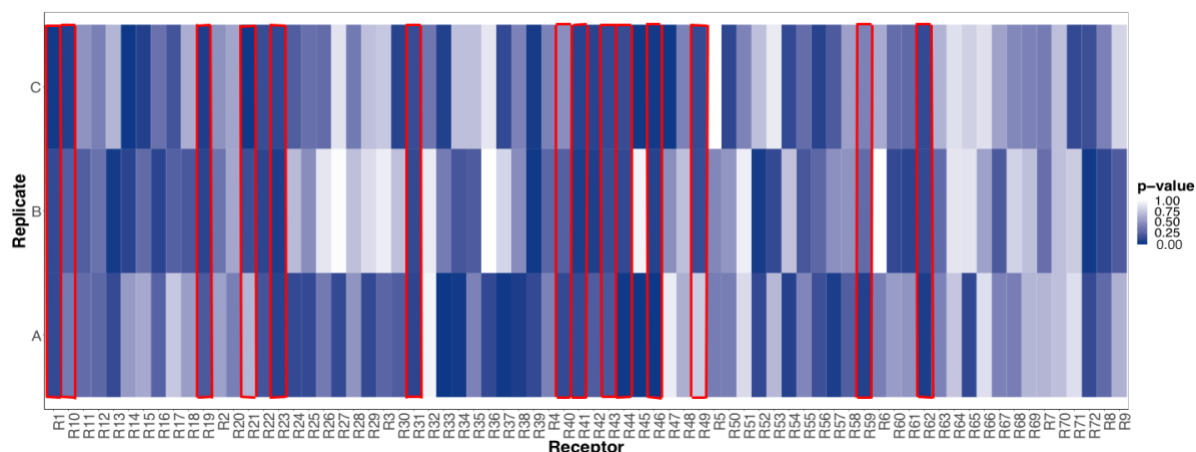


Figure 3: Heat Map Showing Significance Levels Between Amino Acid Treatment and Vehicle for the Lipid Metabolism GPCRs. The significance levels (p -values), ranging between 0.00 (dark blue) to 1.00 (white), between the 4X essential 8X non-essential amino acid (4/8X aa) mixture and Opti-MEM vehicle of the 72 lipid metabolism GPCRs in the three biological replicates (A, B, C) of the high-throughput screen. The receptors whose activities were significantly altered by the amino acid mixture (described in Figure 1) are outlined in red.

Of the 14 receptor candidates, MC4, DP2, CCK1, GPBA, S1P1, and S1P4 were chosen as the 6 receptor candidates that would be used for further investigations, due to their greater consistency (Fig 3) and magnitude of fold changes (Fig 2C) between the 4/8X aa treatment and VEH across the three biological replicates.

L-Phenylalanine activates MC4, DP2, GPBA, S1P1, and S1P4

In order to identify which of the 19 *L*-amino acids present in the 4/8X aa mixture was altering the activity of the 6 receptor candidates (MC4, DP2, GPBA, CCK1, S1P1, S1P4), HTLA cells were transfected with one of the 6 receptors and treated with the 4X essential amino acid mixture (E), the 8X non-essential amino acid mixture (NE), the 4/8X aa mixture, or VEH (Fig. 4). Treatment of the positive control LPAR1 cells with 10% FBS resulted in significantly increased RLU/A420 when compared to VEH, with an average fold change relative to VEH of 14 ± 1 (Fig. 4A).

The essential amino acid mixture appeared to contain the amino acid responsible for the significant differences in RLU/A420 reported in the HTS for each of the 6 receptor candidates (Fig. 4B). For MC4, the RLU/A420 of the 4/8X aa mixture, and the E treated cells did not significantly differ from VEH, but did correspond to fold changes relative to VEH of 1.7 ± 0.1 , and 1.6 ± 0.3 , respectively. Importantly, the RLU/A420 of the NE treated MC4 cells was significantly lower than the 4/8X aa mixture treated MC4 cells, indicating that the NE mixture did not contain the amino acid of interest. For DP2, the RLU/A420 of the E treated cells was significantly increased compared to VEH and NE treated cells, with a fold change relative to VEH of 3.4 ± 0.8 . The RLU/A420 of the NE treated DP2 cells did not differ from VEH. For GPBA, there was no significant difference in RLU/A420 of the E treated, and 4/8X aa mixture treated cells compared to VEH treated cells. However, the 4/8X aa mixture, and the E treatments corresponded to fold changes relative to VEH of 2.9 ± 0.8 , and 2.9 ± 0.6 , respectively. Importantly, the RLU/A420 of the NE treated GPBA cells was significantly decreased compared to VEH, 4/8X aa mixture, and E treated cells, again suggesting the NE mixture does not contain the amino acid of interest. In contrast to the other 5 receptor candidates, for CCK1 we would expect to see a decrease in RLU/A420 in the treatment condition containing the amino acid of interest. There was no significant difference in RLU/A420 between the 4/8X aa, and E treated CCK1 cells compared to VEH, but these treatment conditions did correspond to fold changes relative to VEH of 0.54 ± 0.09 , 0.50 ± 0.08 , respectively. Furthermore, RLU/A420 of the NE treated CCK1 cells was significantly greater than that of the 4/8X aa mixture, and E treated cells, but did not differ from VEH. This suggests the NE mixture did not contain the amino acid of interest. For S1P1, the RLU/A420 of

the 4/8X aa mixture, the E, and the NE treated S1P1 cells were significantly greater compared to the VEH treated cells. Important to note, the fold change relative to VEH of NE treated S1P1 cells is only 1.1 ± 0.1 , while that of the 4/8X aa and E treated S1P1 cells is 1.9 ± 0.3 , and 2.7 ± 0.4 , respectfully. This suggests that the statistically significant increase in RLU/A420 of the NE treated cells compared to VEH is not biologically significant. Finally, for S1P4, the RLU/A420 of the E treated cells is significantly greater than that of the VEH, 4/8X aa mixture, and NE treated cells and corresponds to a fold change relative to VEH of 2.6 ± 0.4 . The RLU/A420 of the NE treated S1P4 cells did not significantly differ from VEH.

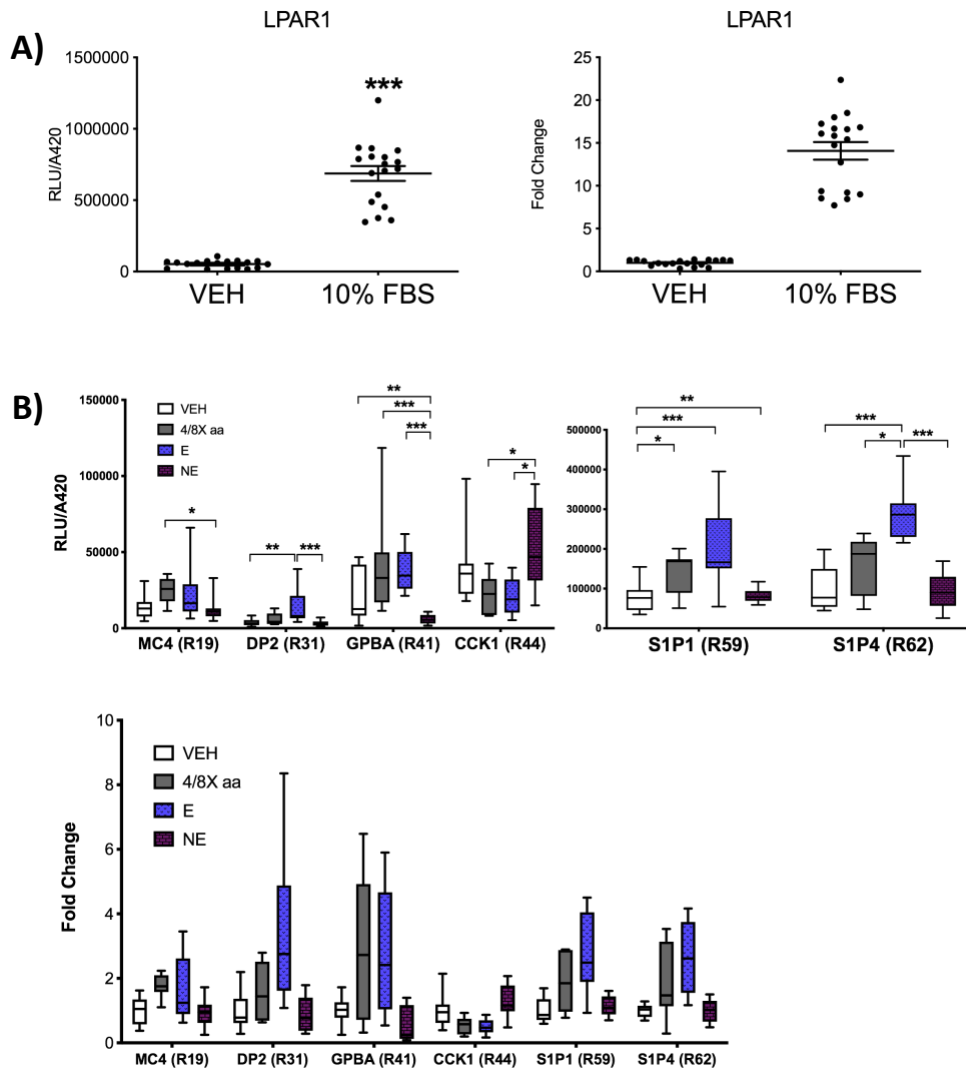


Figure 4: Essential Amino Acids Alter the Activity of the 6 Receptor Candidates.

Receptor activation was measured following a PRESTO-TANGO β -arrestin recruitment assay. HTLA cells were transiently transfected with GPCR PRESTO TANGO plasmids as indicated. **A)** The relative luminescence units (RLU) adjusted by β -galactosidase expression (absorbance at 420 nm; Left), and fold change RLU/A420 (Right) of the positive control lysophosphatidic acid 1 (LPAR1) PRESTO TANGO receptor treated with Opti-MEM vehicle (VEH) and 10% fetal bovine serum (FBS). **B)** The RLU/A420 (Top) and fold change (Bottom) of the 6 receptor candidates treated with Opti-MEM VEH (white), the 4X essential 8X non-essential amino acid (4/8X aa) mixture (grey), the 4X essential amino acid mixture (E; purple with dots), and the 8X non-essential amino acid mixture (NE; pink with bricks). Note the different range in RLU/A420 for the two sets of receptors. All box plots are shown as highest and lowest values; scatter plots represent individual data points with mean and SEM shown. Statistical significance (* $P < 0.05$; ** $P < 0.001$; *** $P < 0.0001$) was evaluated using parametric one-way ANOVAs with Bonferroni post-hoc tests on log₁₀ transformed RLU/A420 data of each receptor from all three sets combined with outliers removed. The non-parametric Mann-Whitney U test was used for the LPAR1 RLU/A420 data.

The data thus demonstrates that for each of the 6 receptor candidates, the essential amino acid mixture contained the amino acid(s) responsible for the significant increase (or decrease for CCK1) in RLU/A420 compared to VEH reported in the HTS experiment. Next, each receptor candidate was treated with the 12 essential amino acids individually, at the concentrations corresponding to those of the 4X essential amino acid mixture (Fig. 5). Treatment of the positive control LPAR1 cells with 10% FBS resulted in significantly greater RLU/A420 compared to VEH, with a fold change relative to VEH of 15.9 ± 0.7 (Fig. 5A).

Remarkably, when compared to VEH, the *L*-Phe treatment significantly increased RLU/A420 of cells expressing MC4, DP2, GPBA, S1P1, and S1P4, but not CCK1 (Fig 5B-G). This corresponded to fold changes of *L*-Phe relative to VEH of 2.2 ± 0.2 , 2.7 ± 0.5 , 3.2 ± 0.3 , 2.9 ± 0.3 and 2.2 ± 0.3 fold for MC4, DP2, GPBA, S1P1, and S1P4, respectively. Importantly, for each receptor, the RLU/A420 of the other 11 essential amino acids did not significantly differ from VEH, except for *L*-Cysteine (Cys) treatment which resulted in significantly decreased RLU/A420 compared to VEH for all receptors except GPBA. A420 values for all Cys treatments were also reduced compared to VEH A420 (data not shown) suggesting this decrease in activity is due to Cys toxicity and not inhibitory action of Cys at the receptors. Interestingly, *L*-Phe treatment did not significantly alter RLU/A420 of CCK1 expressing cells (fold change relative to VEH of 1.0 ± 0.1). Importantly, it is reasonable to presume that the significant decrease in RLU/A420 of Cys treated CCK1 expressing cells compared to VEH is due to toxicity, as this was the case for the other 5 receptor candidates.

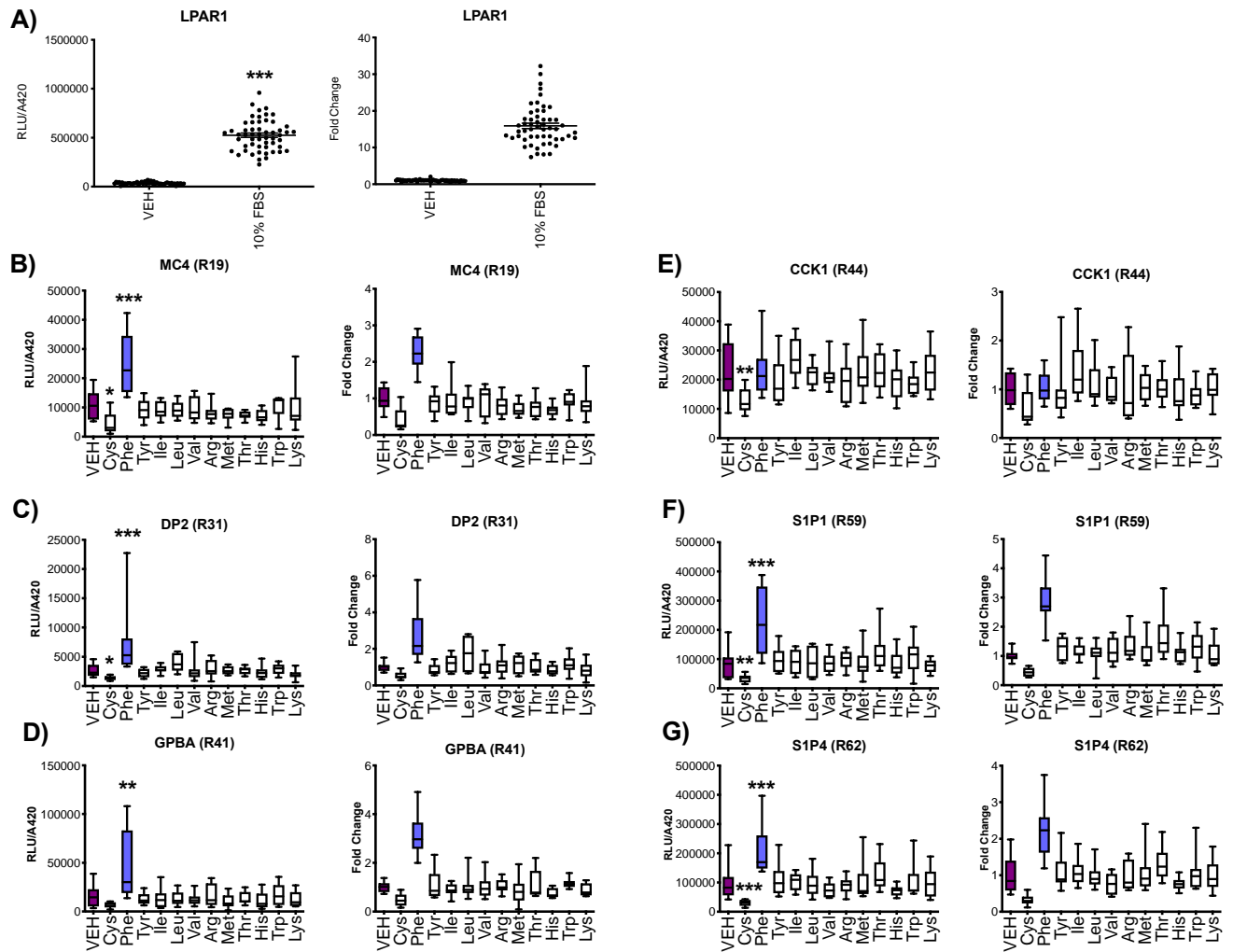


Figure 5: L-Phe Significantly Activates MC4, DP2, GPBA, S1P1, and S1P4. Receptor activation was measured following a PRESTO-TANGO β -arrestin recruitment assay. HTLA cells were transiently transfected with GPCR PRESTO TANGO plasmids as indicated. **A)** The relative luminescence units (RLU) adjusted by β -galactosidase expression (absorbance at 420 nm; Left), and fold change RLU (Right) of the positive control lysophosphatidic acid 1 (LPAR1) PRESTO TANGO receptor treated with Opti-MEM vehicle (VEH) and 10% fetal bovine serum (FBS). **C-H)** The RLU/A420 (Left) and fold change (Right) between Opti-MEM VEH (pink) and each individual essential amino acid (Concentrations in mM: 2.9 *L*-Arg HCl, 1.0 *L*-Cys 2HCl, 1.0 *L*-His HCl H₂O, 1.6 *L*-Ile, 1.6 *L*-Leu, 2.0 *L*-Lys HCl, 0.4 *L*-Met, 0.8 *L*-Phe, 1.6 *L*-Thr, 0.2 *L*-Trp, 0.8 *L*-Tyr, and 1.6 *L*-Val) with *L*-Phe shown in purple, for MC4 (**C**), DP2 (**D**), GPBA (**E**), CCK1 (**F**), S1P1 (**G**), and S1P4 (**H**). All box plots are shown as highest and lowest values; scatter plots represent individual data points with mean and SEM. Statistical significance (* $P < 0.05$; ** $P < 0.001$; *** $P < 0.0001$) was evaluated using parametric one-way ANOVAs with Bonferroni post-hoc test on log₁₀ transformed RLU/A420 data of each receptor from all three sets combined with outliers removed. The non-parametric Mann-Whitney U test was used for the LPAR1 RLU/A420 data, and to compare S1P4 Trp to S1P4 VEH. The non-parametric Kruskal-Wallis test with Dunnet post hoc tests was used to compare MC4 Cys and Trp to VEH.

Overall it was found that *L*-Phe significantly increased the activity of 5 lipid metabolism GPCRs: MC4, DP2, GPBA, S1P1, and S1P4. Importantly, *L*-Phe does not alter the activity of CCK1. The toxicity of the *L*-Cys treatment likely accounts for the decrease in RLU/A420 observed for CCK1 in the HTS and NE v E experiments as this treatment condition was toxic to the MC4, DP2, S1P1, and S1P4 expressing cells, and resulted in decreased A420 values.

DISCUSSION

Given the growing body of literature suggesting metabolites are important signaling molecules⁴, and that amino acids, in particular, modulate energy homeostasis at amino acid sensing receptors (i.e. taste receptors⁴¹, CaR⁵³, HCA³⁵⁵), this study aimed to investigate whether monomeric amino acids activate GPCRs involved in lipid metabolism. This was achieved by employing a High-Throughput Screen (HTS) approach in which 19 monomeric amino acids were screened against 72 lipid metabolism GPCRs and receptor activity was measured using the PRESTO TANGO assay (Fig. 1). In the HTS, the 4/8X aa treatment significantly increased (or decreased for CCK1) the RLU/A420 of 14 lipid metabolism GPCRs, compared to VEH. Following evaluation of the consistency and magnitude of this difference, 6 receptors were chosen for further experimentation: MC4, DP2, GPBA, CCK1, S1P1, and S1P4. The essential amino acid mixture was subsequently shown to contain the amino acid of interest for all 6 receptor candidates. Finally, through investigating the 12 essential amino acids present in the 4X essential amino acid mixture, it was found that *L*-Phe activated MC4, DP2, GPBA, S1P1, and S1P4, but not CCK1.

The PRESTO TANGO assay is a proximity assay that measures receptor activity in terms of β -arrestin recruitments^{57,58}. An increase in RLU/A420 results from increased luciferase expression following recruitment of the β -arrestin-TEV protease fusion protein to the activated GPCR-TEV cleavage site-tTA fusion protein and subsequent release of the tTA that travels to the nucleus and increases luciferase expression (Fig. 1A)^{57,58}. In this way, the significantly increased RLU/A420 of the 4/8X aa mixture treated A1, BLT1, MC4, DP2, GPBA, GPR1, GPR6, EP3, OXGR1, FFA1, FFA4, S1P1, and S1P4 expressing cells, when compared to VEH, indicates that an amino acid present in this mixture was activating these receptors. This is supported by the use of the positive control LPAR1 expressing cells in each experiment. LPAR1 is activated by LPA which is found in serum^{59–61}. In each experiment, the RLU/A420 of 10% FBS treated LPAR1 expressing cells were robustly and significantly increased compared to VEH (Fig. 2A, 4A, 5A). The PRESTO TANGO assay was thus effective in measuring receptor activation, although with a non-negligible degree of variability being noted.

Since MC4, DP2, GPBA, CCK1, S1P1, and S1P4 were found to be more consistently activated by the 4/8X aa treatment across the three biological replicates (Fig. 3), and this translated to greater fold changes in RLU/A420 relative to VEH (Fig. 2), these receptors were chosen for further experimentation. Importantly, the other 8 lipid metabolism GPCRs, A1, BLT1, GPR1, GPR6, EP3, OXGR1, FFA1, and FFA4 merit further research in order to evaluate whether *L*-Phe, or another amino acid, is activating these receptors. Furthermore, many receptors (GPR65, GPR68, GPR34, GPR183, CCK2, LPA5, CysLT2, GPR3, CMKLR1, HCA2, beta3, OXER1, FPR2, GPR65, and FFA2) were found to be significantly activated by the 4/8X aa mixture in at least one set of the

HTS (Fig. 3). Although this activation was not sufficiently robust when all three sets were analyzed together, this finding raises the possibility that amino acids may have a global effect on a large array of GPCRs in order to fine tune energy homeostasis. Future studies will thus need to assess whether treatment with *L*-Phe alone results in more consistent activation of these receptors.

Critically, the Opti-MEM used as VEH for amino acid treatments in all experiments contained 0.18-0.21 mM *L*-Phe. This may have resulted in slightly activated receptors in the VEH conditions that would translate to underestimated fold changes. This may partially account for the lack of significant increase in RLU/A420 of E treated MC4, DP2, and GPBA expressing cells compared to the respective VEHs (Fig. 4). For these receptors, a significantly decreased RLU/A420 in NE treated cells relative to 4/8X aa treatment (MC4), E treatment (DP2), or all treatments (GPBA), was sufficient to justify moving forward with only essential amino acids (Fig. 4). Furthermore, the RLU/A420 of 4/8X aa treatments and E treatments were not significantly different for MC4, DP2, CCK1, GPBA, S1P1 or S1P4, which is reflected in similar fold changes.

In the HTS, the 4/8X aa treatment significantly decreased the RLU/A420 of CCK1 expressing cells compared to VEH (Fig. 2). Similarly, the RLU/A420 of the E treated CCK1 expressing cells was significantly decreased compared to NE treated cells, and did not differ from the 4/8X aa treatment (Fig. 4). Taken together, we suggest three potential explanations: (1) An essential amino acid was acting as an inverse agonist and decreasing the constitutive activity of CCK1, (2) a component in Opti-MEM was activating CCK1, and an essential amino acid was acting as an antagonist and inhibiting this effect, or finally (3) an essential amino acid was toxic and causing a decrease in cell

number and/or protein expression resulting in lower RLU/A420 values. Upon further investigation, it was found that *L*-Cys treatment significantly reduced the RLU/A420 of MC4, DP2, S1P1, S1P4, and CCK1 expressing cells, compared to the respective VEHs (Fig. 5), and that this was accompanied by abnormally low A420 values for each receptor (data not shown). This strongly suggests that Cys was toxic and caused a decrease in cell number and/or protein expression in CCK1 treated cells during the HTS and NE v E experiments.

Remarkably, when MC4, DP2, CCK1, GPBA, S1P1, and S1P4 expressing cells were treated with the individual essential amino acids, it was found that only *L*-Phe treatment significantly increased RLU/A420 compared to VEH for each receptor except CCK1. This indicates that 0.8 mM *L*-Phe activated MC4, DP2, GPBA, S1P1, and S1P4 with fold changes in RLU/A420 relative to VEH from 2.2 to 3.2. Since *L*-Phe was found to be the sole amino acid that activated these receptors, it could be argued that *L*-Phe was somehow interacting with the PRESTO TANGO assay independent of the receptors. For example, *L*-Phe may somehow increase the luminescent reaction catalyzed by luciferase. However, if this was the case, one would expect that all 72 lipid metabolism GPCRs, and not only 14, would have had significantly increased RLU/A240 compared to VEH upon treatment with the *L*-Phe containing 4/8X aa mixture in the HTS. Furthermore, CCK1 acted as a convenient control for this possibility, as CCK1 expressing cells were treated identically to the other 5 receptor candidates, and *L*-Phe treatment did not significantly increase RLU/A420 when compared to VEH (Fig. 5). Accordingly, the fold change in RLU/A420 of *L*-Phe treated CCK1 expressing cells relative to VEH was 1.0 ± 0.1 . Together, these data argue that *L*-Phe was directly activating MC4, DP2, GPBA, S1P1,

and S1P4, which triggered β -arrestin recruitment and thus increased the expression of luciferase.

L-Phe is an essential aromatic amino acid that is abundant in and must be derived from dietary protein^{62,63}. In ad-libitum fed and fasted rats, plasma *L*-Phe concentrations range from $155 \pm 1 \mu\text{M}$, and $121 \pm 4 \mu\text{M}$, respectively⁶⁴. In humans, the normal plasma level of *L*-Phe is 0.061 mM, and can reach over 1.21 mM in patients with phenylketonuria (PKU) a disease in which phenylalanine metabolism is disrupted⁶⁵. In this study, *L*-Phe was applied to cells at 0.8 mM, which is above normal plasma levels. However, *L*-Phe is likely at much higher concentrations in the lumen of the gut following consumption of a meal. Indeed, studies investigating *L*-Phe's effects on colonic L-cells isolated from mice used concentrations up to 100 mM⁶³, suggesting the concentration used in this study is still physiologically relevant.

Our finding that *L*-Phe activated 5 receptors involved in energy homeostasis is not entirely surprising given *L*-Phe's highly regulated metabolism^{66,67}, together with its emerging role in regulating energy homeostasis^{63,68,69}. *L*-Phe metabolism is highly regulated as it is required for tyrosine and protein synthesis^{66,67}, and becomes toxic at high concentrations^{67,70}. Following ingestion of a protein containing meal, proteins are broken down in the gastrointestinal lumen and intestinal enterocytes into individual amino acids which are transported into hepatic portal circulation⁷¹. The transport of aromatic amino acids into circulation and subsequently into tissues such as the liver and kidney is facilitated by the T-type aromatic amino acid transporter TAT1⁷¹. Since the liver is the major site of *L*-Phe metabolism, this organ plays an integral role in regulating *L*-Phe availability in the plasma⁷². Indeed, increased levels of plasma aromatic amino

acids, including *L*-Phe, are correlated with the severity of liver diseases⁷³. In the absorptive state following protein ingestion, 50% of *L*-Phe is channeled into the liver for use in protein synthesis, or oxidation to *L*-Tyr by phenylalanine hydroxylase (PAH)^{71,74}. During the post-absorptive state, *L*-Phe is derived from protein breakdown and 15% is oxidized to *L*-Tyr⁷². Conversion of *L*-Phe to *L*-Tyr enables the liver to fine-tune plasma *L*-Phe levels in order to satisfy protein synthesis requirements, while preventing toxicity associated with elevated plasma *L*-Phe levels⁶⁷. The importance of proper *L*-Phe metabolism is exemplified in the disease PKU. PKU is characterized by a loss of function mutation in PAH resulting in growth failure, microcephaly, seizures, and intellectual impairments due to toxic levels of *L*-Phe and its by products, and a deficiency in *L*-Tyr derived neurotransmitters (NT)⁶⁷.

In this study, it was found that *L*-Phe activated MC4 and S1P1 which have been shown to be highly expressed in the CNS^{1,75}. It is important then to consider to what extent *L*-Phe may act as a signaling molecule in the brain. Plasma *L*-Phe levels dictate the entry of *L*-Phe into the brain, where normal levels fall between 50 and 100 μM , which has important implications for the biosynthesis of serotonin and catecholamine NTs⁶⁶. *L*-Phe, *L*-Tyr, BCAAs, and *L*-Trp compete for access to the CNS as they are all transported across the blood brain barrier (BBB) by the large neutral amino acid (LNAA) carrier, for which the amino acids' K_m values are approximately their concentration in the plasma⁶⁶. As such, an increase in plasma *L*-Phe levels allows *L*-Phe to outcompete other LNAAs, such as *L*-Tyr, for transport into the CNS, thereby interfering with brain function due to altered NT biosynthesis⁶⁶. *L*-Phe can itself be used as a precursor for catecholamine NT synthesis since it is a substrate for tyrosine hydroxylase (TH), an enzyme that converts *L*-

Tyr to L-DOPA, the rate limiting step of catecholamine synthesis⁶⁶. However, *L*-Tyr is the preferred substrate for TH such that levels of *L*-Tyr dictate TH activity⁶⁶. Importantly, following a meal, there is an increase in plasma *L*-Tyr and *L*-Phe levels⁷⁰ such that the concentration of these amino acids increases in the brain which alters TH activity and so catecholamine synthesis⁶⁶. Since hypothalamic catecholamine synthesizing neurons are involved in food intake, altered levels of aromatic amino acids in the brain may act as a signal of dietary protein levels to the hypothalamic circuitry involved in food intake⁶⁶. With this being said, *L*-Phe's role in regulating energy homeostasis goes far beyond modifying catecholamine biosynthesis.

In this study, it was found that *L*-Phe activated 5 receptors involved in lipid metabolism and general energy homeostasis. The importance of amino acids in regulating energy homeostasis has become increasingly clear with a growing body of literature demonstrating that high protein diets (20-30% protein), when compared to control isocaloric diets, induce acute⁷⁶ and long lasting satiety⁷⁷, and are associated with increased weight loss⁷⁰. Importantly, it appears that monomeric amino acids acting at amino acid sensing receptors are mediating the satiating effects of high protein diets^{63,70}. In agreement with this study's findings, *L*-Phe in particular has been shown to play an important role in amino acid mediated changes in food intake, energy expenditure, hormone release, glucose homeostasis, and upper GI motor function^{63,69}. A recent study by Alamshah *et al.* (2017) showed that intra-ileal (10 mM) and oral *L*-Phe (3 mmol/kg) administration in fasted and ad-libitum fed rats resulted in decreased food intake and increased energy expenditure⁶³. Furthermore, 30 mM *L*-Phe was shown to increase the release of the satiety and incretin hormone glucagon-like peptide 1 (GLP-1) from the

intestinal secretin tumor cell line 1 (STC-1). Additionally, 10 and 100 mM *L*-Phe increased GLP-1 release, and 50 and 100 mM *L*-Phe increased release of the satiety hormone peptide YY (PYY) from colonic L-cells isolated from mice⁶³. *L*-Phe was also shown to increase plasma insulin and decrease plasma glucose levels in rats following an intraperitoneal glucose tolerance test⁶³. Importantly, these effects were shown to be partially mediated by the aromatic amino acid sensing receptor CaR⁶³. Another study by Steinert *et al.* (2015) demonstrated that intraduodenal administration of *L*-Phe (0.45kcal/min) significantly decreased antral pressure and increased phasic pyloric pressure of the upper GI tract, and increased CCK release in a dose dependent and time specific manner⁶⁹. Importantly, administration of *L*-Gln did not alter gut motility or hormone release suggesting that these are specific functions of *L*-Phe, and not amino acids in general⁶⁹. This further supports the notion of amino acid sensing receptors contributing to the satiating effects of high protein diets, as these receptors would have different affinities for structurally distinct amino acids. This agrees with the findings of this study that out of the 19 amino acids, only *L*-Phe activated 5 receptors involved in energy homeostasis.

In further support of this study's finding that *L*-Phe is a signaling molecule at several GPCRs, *L*-Phe is already a known agonist for the amino acid sensing receptors CaR, GPR142, and GPR139^{63,64,68,78}. CaR is expressed throughout the GI tract, including enteroendocrine cells of the colon⁶⁸. *L*-Phe's effects on food intake, GLP-1, PYY, and CCK release are at least partially mediated by CaR, for which it is a potent agonist^{63,68}. Importantly, inhibiting CaR only partially reduces *L*-Phe induced GLP-1⁶³ and CCK

release⁶⁸ suggesting *L*-Phe may act at other receptors to mediate the previously reported effects.

L-Phe is also an agonist of the closely related orphan GPCRs GPR142 and GPR139 which share 50% amino acid identity and 67% homology, but have markedly different expression profiles; GPR139 is exclusively expressed in the CNS, while GPR142 is widely expressed in peripheral organs, most notably in the pancreas^{64,79}. A recent study has shown that GPR142 increases cAMP in pancreatic β -cells ultimately increasing cell viability, inhibiting apoptosis, and potentiating glucose stimulated insulin release via a PKA pathway⁷⁸. Lin *et al.* (2016) demonstrated that *L*-Phe induced insulin secretion was significantly reduced in GPR142 KO mice, but that the magnitude of this difference was small, and GPR142 KO mice were still able to suppress glucose excursion. However, *L*-Phe induced gastric inhibitory peptide (GIP) release was blunted in GPR142 KO mice⁵⁴. Taken together, these findings suggest that *L*-Phe acting at GPR142 mediates secretion of metabolic hormones⁵⁴. However, *L*-Phe must also be acting elsewhere to alter glucose homeostasis⁵⁴. Perhaps this is simply *L*-Phe activating CaR, however further research is required to assess whether CaR and GPR142 account for all of *L*-Phe's aforementioned effects on energy homeostasis. The results from this study strongly suggest that *L*-Phe has a more widespread effect on many GPCRs involved in energy homeostasis than previously thought.

As for the orphan receptor GPR139, *L*-Phe and *L*-Trp are both agonists and share a common binding site^{64,80}. Little is known of the physiological role of GPR139, however, given its expression in the striatum, hypothalamus, and habenula, GPR139 is thought to play an important role in locomotor activity, metabolism, addiction, and mediating the

intellectual disabilities of individuals suffering from PKU⁸¹. Interestingly, GPR139 has been shown to be activated by agonists of melanocortin receptors released from POMC neurons, those being ACTH, α -MSH and β -MSH⁸¹. This further supports the notion that this receptor may be involved in regulating energy homeostasis through interacting with the central melanocortin system. The activity of *L*-Phe at GPR139 is important for this study in several ways. First, it demonstrates that *L*-Phe is already known to act as a signalling molecule at GPCRs in the brain. Secondly, this demonstrates the link between *L*-Phe and the melanocortin system for which it was found to activate the main component: MC4. Along with the previously mentioned role of *L*-Phe in NT biosynthesis, these findings make a strong case for the role of *L*-Phe as a signalling molecule regulating energy homeostasis at the level of the CNS, and support this study's finding that *L*-Phe activates MC4 and S1P1.

As was previously described, MC4 is activated by derivatives of POMC that are released from POMC neurons of the arcuate nucleus and the nucleus of the solitary tract^{1,34,35}. In the brain, MC4 is highly expressed in the paraventricular nucleus (PVN) and the dorsal motor nucleus of the vagus (DMV). Activation of the central melanocortin system decreases food intake and increases energy expenditure^{1,34,36}. MC4 is also involved in regulating GI function as it is expressed on efferent and afferent vagal nerves that regulate GI function, as well as being expressed in the DMV and NTS where vagal efferent and afferent nerves project to, respectively⁸². Furthermore, a study by Panaro *et al.* (2014) revealed that MC4 is also expressed on the basolateral membrane of GLP-1/PYY positive L-cells of the GI tract⁸². In general, activation of MC4 expressed on GLP-1/PYY positive L-cells by exogenous application of MC4 agonists increases the

release of PYY and GLP-1 which then decrease intestinal epithelial Cl⁻ secretion and gut motility⁸². Importantly, the endogenous ligand responsible for MC4 activation in the GI tract is currently unknown⁸². This supports this study's finding that *L*-Phe activated MC4, since *L*-Phe induces GLP-1 and PYY release from enteroendocrine cells of the GI tract⁶³.

S1P1 is coupled to G_{i/o} and thus inhibits adenylate cyclase (AC) and activates PLC, MAPK, Rac, and intracellular Ca²⁺ mobilization which allows for cellular aggregation and migration¹⁹. S1P1 is widely expressed and is involved in regulating cellular processes in the spleen, heart, lung, adipose tissue, liver, thymus, kidney, and skeletal muscle^{19,83}. Silva *et al.* (2014) demonstrated the importance of S1P1 in regulating the hypothalamic neuro-circuitry involved in energy homeostasis. The authors demonstrate that S1P1 is highly expressed in POMC neurons, and not AgRP/NPY neurons, of the arcuate nucleus, when compared to peripheral organs⁷⁵. Briefly, activation of S1P1 was associated with an increase in the leptin signalling pathway JAK2/STAT3 which resulted in increased expression of POMC mRNA in POMC neurons of the arcuate nucleus⁷⁵. Consistent with this finding, activation of the S1P1/JAK2/STAT3 pathway was shown to decrease food intake and increase energy expenditure, an effect that required the melanocortin system⁷⁵.

These findings paint an interesting picture in which *L*-Phe may be an important modulator of the melanocortin system. In this study *L*-Phe was shown to activate MC4 and S1P1, both of which are involved in the melanocortin system. Furthermore, other studies have demonstrated that *L*-Phe induces increased energy expenditure, decreased food intake, and increased release of GLP-1, PYY, and CCK^{63,69}; all of which are also mediated by the melanocortin system^{1,82}. Even more convincing, *L*-Phe is a known

agonist of the potential α -MSH receptor GPR139⁸¹. Taken together, these findings suggest that *L*-Phe may play a role in modulating the central and peripheral melanocortin system both directly and indirectly to regulate energy homeostasis. Future studies should thus investigate this possibility directly.

L-Phe was also shown to activate the bile acid receptor GPBA. Since GPBA is highly expressed in the gallbladder epithelium, ileum, colon, liver, BAT and skeletal muscle, and has notable expression in the CNS²², this receptor is an excellent candidate for sensing *L*-Phe. GPBA is coupled to G_s such that activation increases cAMP and activates PKA²². Gallbladder epithelium GPBA alters chloride secretion and the size of the bile acid pool which ultimately alters the absorption of dietary lipids²². Furthermore, GPBA activation in high fat diet-fed mice induces weight loss via a thyroid hormone receptor mediated increase in energy expenditure^{22,84}. GPBA activity also modulates triglyceride and glucose metabolism by inducing GLP-1 secretion from STC-1 cells^{22,85}. These finding thus support the activation of GPBA by *L*-Phe reported in this study since *L*-Phe is known to increase energy expenditure and GLP-1 release⁶³.

L-Phe was also shown to activate S1P4, and DP2, two receptors that appear to be highly involved in the immune system. S1P4 has a low amino acid similarity to S1P1, and is coupled to $G_{i/o}$, $G_{12/13}$, and G_s and thus activates AC, MAPK, PLC, RhoA, and Ca^{2+} mobilization which mediates cytoskeletal rearrangement and cell motility¹⁹. S1P4 is only expressed in the lymph node, spleen, lung, thymus, and immune cells¹⁹. S1P4 is not understood as well as S1P1, however, given its expression profile, it has been suggested to modulate the functioning of the immune system⁸⁶. For example, S1P4 regulates the

expression of various receptors on immune cells, and triggers neutrophil activation and migration⁸⁶.

DP2 is activated by the prostaglandin PGD₂⁸⁷ and is coupled to G_{i/o}⁸⁸. Studies investigating PGD₂ signaling at DP2 have mainly focused on DP2's role in eosinophil chemotaxis as it is highly expressed on Th2 cells⁸⁹. Indeed DP2 appears to play a significant role in mediating inflammatory processes in several tissues including the lungs, kidneys, GI tract, and central nervous system, and is expressed on several cells of the immune system including mast cells, macrophages, eosinophils, basophils, and dendritic cells, as well as bronchial epithelial cells⁸⁹. Interestingly, a study by Wakai *et al.* (2017) found that DP2 was highly expressed in adipocytes, where it enhanced adipogenesis and inhibited lipolysis. This was achieved by DP2 increasing the expression of adipogenic genes and inhibiting the cAMP dependant activation of PKA which inhibits the stimulatory phosphorylation of hormone sensitive lipase (HSL) that mediates lipolysis⁸⁸. In this way, DP2 is involved in lipid accumulation – an important aspect of adipocyte differentiation⁸⁸. Taken together, *L*-Phe activation of DP2 and S1P4 may allow for the coordination of amino acid metabolism with the immune system and lipid metabolism, a possibility that future studies should investigate.

This study chose the β -arrestin recruitment PRESTO TANGO assay to measure receptor activation as it is independent of coupling to G proteins and downstream signal transduction pathways^{6,10}. The PRESTO TANGO assay was especially useful given the high throughput nature of this study in which the 72 lipid metabolism GPCRs differed greatly in their coupling to G proteins. With this being said, the limitations of the PRESTO TANGO assay are that it has an intrinsic degree of variability, and does not

provide information on the physiological relevance of receptor activation. Future studies must therefore confirm *L*-Phe's actions at MC4, DP2, GPBA, S1P1, and S1P4 by using a more physiologically relevant assay system (e.g. Ca²⁺ mobilization, cAMP accumulation, phosphorylation of downstream effectors). This is now a task that is made much more feasible given the receptors and amino acid have been identified and can now be investigated on an individual basis.

In conclusion, screening 19 monomeric amino acids against 72 GPCRs involved in lipid metabolism revealed 13 amino acid sensing receptor candidates – A1, BLT1, MC4, DP2, GPBA, GPR1, GPR6, EP3, OXGR1, FFA1, FFA4, S1P1, and S1P4. Of these receptors, MC4, DP2, GPBA, S1P1, and S1P4, were chosen for further experimentation and were shown to only be activated by *L*-Phe. Future studies should investigate whether *L*-Phe was also activating the other 8 receptor candidates. *L*-Phe activation of GPBA, MC4, and S1P1 agrees with the literature available on *L*-Phe signaling, as it is known to activate GPCRs with similar expression profiles as these 3 lipid metabolism GPCRs. Furthermore, *L*-Phe's effects on energy homeostasis line up with the activities of GPBA, MC4, and S1P1. In particular, there appears to be a link between *L*-Phe and the melanocortin system which should be investigated directly in future studies. As for DP2 and S1P4, their expression and role in mediating immune cells may represent a link between amino acid metabolism and the immune system, which also represents an important possibility that should be investigated. Overall, the findings from this study suggest that *L*-Phe is an important extracellular signaling molecule at a potentially very large array of GPCRs, which may allow coordination of many different physiological processes with amino acid metabolism. This study has important implications for

research in obesity and the metabolic syndrome as it deepens our understanding of the therapeutic benefits of high protein diets in weight loss and preventing weight gain. Furthermore, it contributes to clarifying the role of metabolites as signaling molecules which will greatly aid in understanding the mechanisms of obesity, the metabolic syndrome, type 2 diabetes, and other diseases.

REFERENCES

1. Nogueiras, R. *et al.* The central melanocortin system directly controls peripheral lipid metabolism. *J. Clin. Invest.* **117**, 3475–3488 (2007).
2. De Vriese, C. & Delporte, C. Influence of ghrelin on food intake and energy homeostasis. *Curr. Opin. Clin. Nutr. Metab. Care.* **10**, 615–619 (2007).
3. Hara, T. *et al.* Role of free fatty acid receptors in the regulation of energy metabolism. *Biochim. Biophys. Acta - Mol. Cell Biol. Lipids.* **1841**, 1292–1300 (2014).
4. Husted, A. S., Trauelsen, M., Rudenko, O., Hjorth, S. A. & Schwartz, T. W. GPCR-Mediated Signaling of Metabolites. *Cell Metab.* **25**, 777–796 (2017).
5. Rosenbaum, D.M., Rasmussen, S.G.F., & Kobilka, B. K. The structure and function of G-protein-coupled receptors. *Nature.* **459**, 356–363 (2019).
6. Black, J. B., Premont, R. T. & Y, Daaka. Feedback Regulation of G Protein-Coupled Receptor Signaling by GRKs and Arrestins. *Semin. Cell Dev. Biol.* **50**, 95–104 (2016).
7. Leach, K., Sexton, P. M. & Christopoulos, A. Allosteric GPCR modulators: taking advantage of permissive receptor pharmacology. *Trends Pharmacol. Sci.* **28**, 382–389 (2007).
8. Civelli, O., Saito, Y., Wang, Z., Nothacker, H. P. & Reinscheid, R. K. Orphan GPCRs and their ligands. *Pharmacol. Ther.* **110**, 525–532 (2006).
9. Fields, T. A. & Casey, P. J. Signalling functions and biochemical properties of pertussis toxin-resistant G-proteins. *Biochem. J.* **321**, 561–571 (1997).
10. Nobles, K. N. *et al.* Distinct phosphorylation sites on the β 2-adrenergic receptor establish a barcode that encodes differential functions of β -arrestin. *Sci. Signal.* **4**, (2011).
11. Offermanns, S. Hydroxy-Carboxylic Acid Receptor Actions in Metabolism. *Trends Endocrinol. Metab.* **28**, 227–236 (2017).
12. Brown, H. A. & Marnett, L. J. Introduction to lipid biochemistry, metabolism, and signaling. *Chem. Rev.* **111**, 5817–5820 (2011).
13. Fahy, E. *et al.* A comprehensive classification system for lipids. *J. Lipid Res.* **46**, 839–861 (2005).
14. Im, D. S. Intercellular lipid mediators and GPCR drug discovery. *Biomol. Ther.* **21**, 411–422 (2013).
15. Yin, H. *et al.* Lipid G protein-coupled receptor ligand identification using β -arrestin PathHunter™ assay. *J. Biol. Chem.* **284**, 12328–12338 (2009).
16. Morales, P., Isawi, I. & Reggio, P. H. Towards a better understanding of the cannabinoid-related orphan receptors GPR3, GPR6, and GPR12. *Drug Metab. Rev.* **50**, 74–93 (2018).
17. Irving, A. *et al.* Cannabinoid Receptor-Related Orphan G Protein-Coupled Receptors. *Adv. Pharmacol.* **80**, 223-247 (2017).
18. Wymann, M. P. & Schneider, R. Lipid signalling in disease. *Nat. Rev. Mol. Cell Biol.* **9**, 162–176 (2008).
19. Ishii, I., Fukushima, N., Ye, X. & Chun, J. Lysophospholipid Receptors: Signaling and Biology. *Annu. Rev. Biochem.* **73**, 321–354 (2004).
20. Choi, J. W. *et al.* LPA Receptors: Subtypes and Biological Actions. *Annu. Rev.*

- Pharmacol. Toxicol.* **50**, 157–186 (2010).
21. Pagès, C. *et al.* LPA as a Paracrine Mediator of Adipocyte Growth and Function. *Ann. N. Y. Acad. Sci.* **905**, 159–164 (2006).
 22. Pols, T. W. H., Noriega, L. G., Nomura, M., Auwerx, J. & Schoonjans, K. The bile acid membrane receptor TGR5 as an emerging target in metabolism and inflammation. *J. Hepatol.* **54**, 1263–1272 (2011).
 23. Mattern, A., Zellmann, T. & Beck-Sickinger, A. G. Processing, signaling, and physiological function of chemerin. *IUBMB Life.* **66**, 19–26 (2014).
 24. Rourke, J. L., Dranse, H. J. & Sinal, C. J. Towards an integrative approach to understanding the role of chemerin in human health and disease. *Obes. Rev.* **14**, 245–262 (2013).
 25. Goralski, K. B. *et al.* Chemerin, a novel adipokine that regulates adipogenesis and adipocyte metabolism. *J. Biol. Chem.* **282**, 28175–28188 (2007).
 26. Robidoux, J., Martin, T. L. & Collins, S. β -Adrenergic receptors and regulation of energy expenditure: A Family Affair. *Annu. Rev. Pharmacol. Toxicol.* **44**, 297–323 (2004).
 27. Bozaoglu, K. *et al.* Chemerin is associated with metabolic syndrome phenotypes in a Mexican-American population. *J. Clin. Endocrinol. Metab.* **94**, 3085–3088 (2009).
 28. Pulinilkunnil, T. *et al.* Adrenergic regulation of AMP-activated protein kinase in brown adipose tissue in vivo. *J. Biol. Chem.* **286**, 8798–8809 (2011).
 29. Fredriksson, R. & Schiöth, H. B. The repertoire of G-protein-coupled receptors in fully sequenced genomes. *Mol. Pharmacol.* **67**, 1414–1425 (2005).
 30. Fredholm, B. B., Johansson, S. & Wang, Y. Q. Adenosine and the Regulation of Metabolism and Body Temperature. *Adv. Pharmacol.* **61**, 77–94 (2011).
 31. Gnad, T. *et al.* Adenosine activates brown adipose tissue and recruits beige adipocytes via A2A receptors. *Nature.* **516**, 395–399 (2014).
 32. Porkka-Heiskanen, T. & Kalinchuk, A. V. Adenosine, energy metabolism and sleep homeostasis. *Sleep Med. Rev.* **15**, 123–135 (2011).
 33. Cone, R. D. Studies on the physiological functions of the melanocortin system. *Endocr. Rev.* **27**, 736–749 (2006).
 34. Garfield, A. S., Lam, D. D., Marston, O. J., Przydzial, M. J. & Heisler, L. K. Role of central melanocortin pathways in energy homeostasis. *Trends Endocrinol. Metab.* **20**, 203–215 (2009).
 35. Shen, W. jie, Yao, T., Kong, X., Williams, K. W. & Liu, T. Melanocortin neurons: Multiple routes to regulation of metabolism. *Biochim. Biophys. Acta - Mol. Basis Dis.* **1863**, 2477–2485 (2017).
 36. Morrison, S. F., Madden, C. J. & Tupone, D. Central neural regulation of brown adipose tissue thermogenesis and energy expenditure. *Cell Metab.* **19**, 741–756 (2014).
 37. Varela, L. *et al.* Ghrelin and lipid metabolism: Key partners in energy balance. *J. Mol. Endocrinol.* **46**, 43–63 (2011).
 38. Bi, S., Scott, K. A., Kopin, A. S. & Moran, T. H. Differential roles for cholecystinin A receptors in energy balance in rats and mice. *Endocrinology.* **145**, 3873–3880 (2004).
 39. Little, T. J., Horowitz, M. & Feinle-Bisset, C. Role of cholecystinin in appetite

- control and body weight regulation. *Obes. Rev.* **6**, 297–306 (2005).
40. Bröer, S. & Bröer, A. Amino acid homeostasis and signalling in mammalian cells and organisms. *Biochem. J.* **474**, 1935–1963 (2017).
 41. San Gabriel, A. & Uneyama, H. Amino acid sensing in the gastrointestinal tract. *Amino Acids.* **45**, 451–461 (2013).
 42. Brosnan, J. T. Interorgan Amino Acid Transport and its Regulation. *J. Nutr.* **133**, 2068–2072 (2003).
 43. Neis, E. P. J. G. *et al.* Human splanchnic amino-acid metabolism. *Amino Acids.* **49**, 161–172 (2017).
 44. Felig, P., Marless, E., Pozefsky, T. & Cahill, G. Amino Acid Metabolism in the Regulation of Gluconeogenesis in Man. *Am. J. Clin. Nutr.* **23**, 986–992 (1970).
 45. Lynch, C. J. & Adams, S. H. Branched-chain amino acids in metabolic signalling and insulin resistance. **10**, 723–736 (2014).
 46. Closs, E. I., Simon, A., Vékony, N. & Rotmann, A. Plasma Membrane Transporters for Arginine. *J. Nutr.* **134**, 2752S-2759S (2004).
 47. Kavanaugh, M. P. Voltage Dependence of Facilitated Arginine Flux Mediated by the System y⁺ Basic Amino Acid Transporter. *Biochemistry* **32**, 5781–5785 (1993).
 48. Dibble, C. & Manning, B. Signal integration by mTORC1 coordinates nutrient input with biosynthetic output. *Nat Cell Biol.* **15**, 555–564 (2013).
 49. Lackey, D. E. *et al.* Regulation of adipose branched-chain amino acid catabolism enzyme expression and cross-adipose amino acid flux in human obesity. *Am. J. Physiol. - Endocrinol. Metab.* **304**, 1175–1187 (2013).
 50. Morrison, C. D., Reed, S. D. & Henagan, T. M. Homeostatic regulation of protein intake: In search of a mechanism. *Am. J. Physiol. - Regul. Integr. Comp. Physiol.* **302**, (2012).
 51. Nelson, G. *et al.* An amino-acid taste receptor. *Nature* **416**, 199–202 (2002).
 52. Bassoli, A., Borgonovo, G., Caremoli, F. & Mancuso, G. The taste of D- and L-amino acids: In vitro binding assays with cloned human bitter (TAS2Rs) and sweet (TAS1R2/TAS1R3) receptors. *Food Chem.* **150**, 27–33 (2014).
 53. Conigrave, A. D., Quinn, S. J. & Brown, E. M. L-Amino acid sensing by the extracellular Ca²⁺-sensing receptor. *Proc. Natl. Acad. Sci. U. S. A.* **97**, 4814–4819 (2000).
 54. Lin, H. V. *et al.* GPR142 controls tryptophan-induced insulin and incretin hormone secretion to improve glucose metabolism. *PLoS One.* **11**, 1–17 (2016).
 55. Irukayama-Tomobe, Y. *et al.* Aromatic D-amino acids act as chemoattractant factors for human leukocytes through a G protein-coupled receptor, GPR109B. *Proc. Natl. Acad. Sci. U. S. A.* **106**, 3930–3934 (2009).
 56. Kobilka, B. Allosteric activation of the CaR by L-amino acids. *Proc. Natl. Acad. Sci. U. S. A.* **97**, 4419–4420 (2000).
 57. Kroeze, W. K. *et al.* PRESTO-TANGO: an open-source resource for interrogation of the druggable human GPCR-ome. *Nat. Struct. Mol. Biol.* **22**, 362–369 (2015).
 58. Barnea, G. *et al.* The genetic design of signaling cascades to record receptor activation. *Proc. Natl. Acad. Sci. U. S. A.* **105**, 64–69 (2008).
 59. Hama, K., Bandoh, K., Kakehi, Y., Aoki, J. & Arai, H. Lysophosphatidic acid (LPA) receptors are activated differentially by biological fluids: Possible role of

- LPA-binding proteins in activation of LPA receptors. *FEBS Lett.* **523**, 187–192 (2002).
60. Aoki, J. *et al.* Serum lysophosphatidic acid is produced through diverse phospholipase pathways. *J. Biol. Chem.* **277**, 48737–48744 (2002).
 61. Bando, K. *et al.* Lysophosphatidic acid (LPA) receptors of the EDG family are differentially activated by LPA species. Structure-activity relationship of cloned LPA receptors. *FEBS Lett.* **478**, 159–165 (2000).
 62. He, F. *et al.* Functions and Signaling Pathways of Amino Acids in Intestinal Inflammation. *Biomed Res. Int.* **2018**, (2018).
 63. Alamshah, A. *et al.* L-phenylalanine modulates gut hormone release and glucose tolerance, and suppresses food intake through the calcium-sensing receptor in rodents. *Int. J. Obes.* **41**, 1693–1701 (2017).
 64. Liu, C. *et al.* GPR139, an orphan receptor highly enriched in the habenula and septum, is activated by the essential amino acids L-tryptophan and L-phenylalanine. *Mol. Pharmacol.* **88**, 911–925 (2015).
 65. Litwack, G. Metabolism of Amino Acids. in *Human Biochemistry*. 359-393 (Elsevier Inc., 2018).
 66. Fernstrom, J. D. & Fernstrom, M. H. Tyrosine, Phenylalanine, and Catecholamine Synthesis and Function in the Brain. *J. Nutr.* **137**, 1539S-1547S (2007).
 67. Williams, R. A., Mamotte, C. D. S. & Burnett, J. R. Phenylketonuria: an inborn error of phenylalanine metabolism. *Clin. Biochem. Rev.* **29**, 31–41 (2008).
 68. Hira, T., Nakajima, S., Eto, Y. & Hara, H. Calcium-sensing receptor mediates phenylalanine-induced cholecystokinin secretion in enteroendocrine STC-1 cells. *FEBS J.* **275**, 4620–4626 (2008).
 69. Steinert, R. E., Landrock, M. F., Horowitz, M. & Feinle-Bisset, C. Effects of intraduodenal infusions of L-phenylalanine and L-glutamine on antropyloroduodenal motility and plasma cholecystokinin in healthy men. *J. Neurogastroenterol. Motil.* **21**, 404–413 (2015).
 70. Veldhorst, M. *et al.* Protein-induced satiety: Effects and mechanisms of different proteins. *Physiol. Behav.* **94**, 300–307 (2008).
 71. Mariotta, L. *et al.* T-type amino acid transporter TAT1 (Slc16a10) is essential for extracellular aromatic amino acid homeostasis control. *J. Physiol.* **590**, 6413–6424 (2012).
 72. Matthews, D. E. An Overview of Phenylalanine and Tyrosine Kinetics in Humans. *J. Nutr.* **137**, 1549S–1555S (2007).
 73. Gaggini, M. *et al.* Altered amino acid concentrations in NAFLD: Impact of obesity and insulin resistance. *Hepatology* **67**, 145–158 (2018).
 74. Stoll, B., Burrin, D. G., Henry, J. F., Jahoor, F. & Reeds, P. J. Dietary and systemic phenylalanine utilization for mucosal and hepatic constitutive protein synthesis in pigs. *Am. J. Physiol. - Gastrointest. Liver Physiol.* **276**, G49–G57 (1999).
 75. Silva, V. R. R. *et al.* Hypothalamic S1P/S1PR1 axis controls energy homeostasis. *Nat. Commun.* **5**, 1–15 (2014).
 76. Crovetti, R., Porrini, M., Santangelo, A. & Testolin, G. The influence of thermic effect of food on satiety. *Eur. J. Clin. Nutr.* **52**, 482–488 (1998).
 77. Lejeune, M. P. G. M., Westerterp, K. R., Adam, T. C. M., Luscombe-Marsh, N. D.

- & Westerterp-Plantenga, M. S. Ghrelin and glucagon-like peptide 1 concentrations, 24-h satiety, and energy and substrate metabolism during a high-protein diet and measured in a respiration chamber. *Am. J. Clin. Nutr.* **83**, 89–94 (2006).
78. Al-Amily, I. M., Dunér, P., Groop, L. & Salehi, A. The functional impact of G protein-coupled receptor 142 (Gpr142) on pancreatic β -cell in rodent. *Pflugers Arch. Eur. J. Physiol.* **471**, 633–645 (2019).
 79. Süsens, U., Hermans-Borgmeyer, I., Urny, J. & Schaller, H. C. Characterisation and differential expression of two very closely related G-protein-coupled receptors, GPR139 and GPR142, in mouse tissue and during mouse development. *Neuropharmacology.* **50**, 512–520 (2006).
 80. Nøhr, A. C. *et al.* The GPR139 reference agonists 1a and 7c, and tryptophan and phenylalanine share a common binding site. *Sci. Rep.* **7**, 1–9 (2017).
 81. Vedel, L., Nøhr, A. C., Gloriam, D. E. & Bräuner-Osborne, H. Pharmacology and function of the orphan GPR139 G protein-coupled receptor. *Basic Clin. Pharmacol. Toxicol.* **00**, 1–12 (2019).
 82. Ishii, I. *et al.* Selective Loss of Sphingosine 1-Phosphate Signaling with No Obvious Phenotypic Abnormality in Mice Lacking Its G Protein-coupled Receptor, LP B3/EDG-3. *J. Biol. Chem.* **276**, 33697–33704 (2001).
 83. Panaro, B. L. *et al.* The melanocortin-4 receptor is expressed in enteroendocrine l cells and regulates the release of peptide YY and glucagon-like peptide 1 in vivo. *Cell Metab.* **20**, 1018–1029 (2014).
 84. Watanabe, M. *et al.* Bile acids induce energy expenditure by promoting intracellular thyroid hormone activation. *Nature.* **439**, 484–489 (2006).
 85. Katsuma, S., Hirasawa, A. & Tsujimoto, G. Bile acids promote glucagon-like peptide-1 secretion through TGR5 in a murine enteroendocrine cell line STC-1. *Biochem. Biophys. Res. Commun.* **329**, 386–390 (2005).
 86. Olesch, C., Ringel, C., Brüne, B. & Weigert, A. Beyond Immune Cell Migration: The Emerging Role of the Sphingosine-1-phosphate Receptor S1PR4 as a Modulator of Innate Immune Cell Activation. *Mediators Inflamm.* **2017**, (2017).
 87. Carboneau, B. A., Breyer, R. M. & Gannon, M. Regulation of pancreatic β -cell function and mass dynamics by prostaglandin signaling. *J. Cell Commun. Signal.* **11**, 105–116 (2017).
 88. Wakai, E., Aritake, K., Urade, Y. & Fujimori, K. Prostaglandin D2 enhances lipid accumulation through suppression of lipolysis via DP2 (CRTH2) receptors in adipocytes. *Biochem. Biophys. Res. Commun.* **490**, 393–399 (2017).
 89. Jandl, K. & Heinemann, A. The therapeutic potential of CRTH2/DP2 beyond allergy and asthma. *Prostaglandins Other Lipid Mediat.* **133**, 42–48 (2017).

APPENDIX

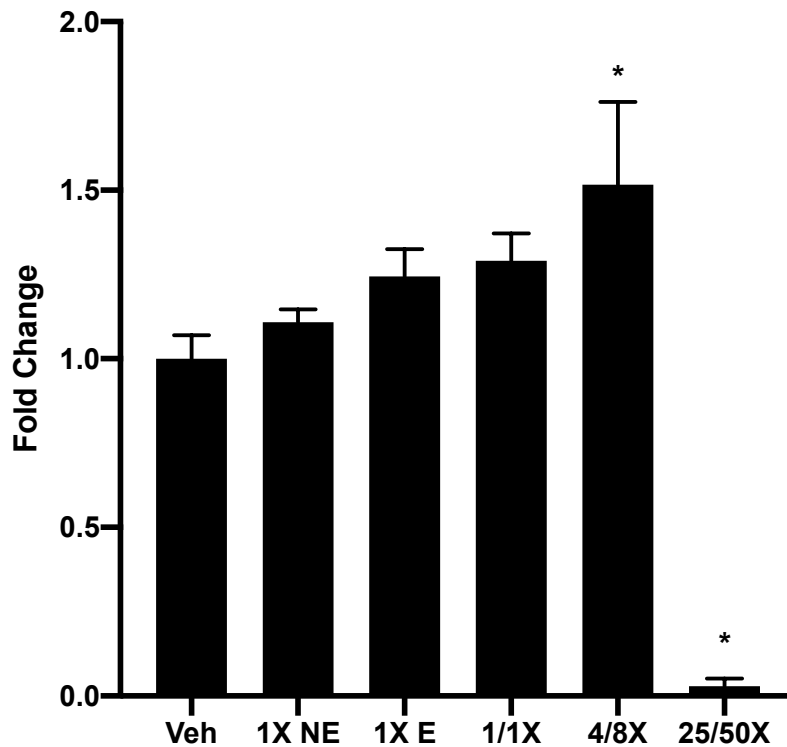


Figure 1: MTT Assay Reveals the 4/8X aa Mixture is Not Toxic. The fold change in absorbance at 570 nm relative to vehicle (Opti-MEM) of the 1X non-essential amino acid mixture (1X NE), 1X essential amino acid mixture (1X E), 1X non-essential 1X essential amino acid (1/1X) mixture, 4X essential 8X non-essential amino acid (4/8X aa) mixture, and the 25X essential 50X non-essential amino acid (25/50X) mixture following a thiazoyl blue tetrazolium bromide (MTT) assay. Statistical significance (* $P < 0.05$) was evaluated using a parametric one-way ANOVA with Bonferroni post-hoc tests. Data courtesy of Madeline Power.

Table 1: Summary of Results from the High Throughput Screen. The significance levels (p -values) between the 4X essential 8X non-essential amino acid (4/8X aa) mixture and Opti-MEM vehicle of the 72 lipid metabolism GPCRs in the three biological replicates (Set A, B, C) of the high throughput screen, and when data from all three sets are combined for analysis. Significance levels were determined using a parametric T-test or non-parametric Mann-Whitney U test (for R1, R41, R62). * $p < 0.05$.

Receptor	A	B	C	All sets combined
R1	0.100	0.099	*0.011	*0.008
R2	0.555	0.328	0.477	0.819
R3	0.248	0.922	0.739	0.448
R4	0.400	0.251	0.400	0.383
R5	0.373	0.429	1.000	0.416
R6	0.386	1.000	0.602	0.489
R7	0.654	0.300	0.370	0.340
R8	0.276	0.081	0.397	0.256
R9	0.633	0.200	0.802	0.586
R10	0.365	0.216	*0.040	*0.006
R11	0.286	0.212	0.486	0.317
R12	0.260	0.319	0.388	0.863
R13	0.106	*0.016	0.653	0.136
R14	0.520	0.071	*0.007	0.730
R15	0.592	0.280	*0.048	0.609
R16	0.232	0.071	0.316	0.108
R17	0.740	0.221	0.157	0.126
R18	0.535	0.178	0.619	0.436
R19	0.186	0.069	*0.036	*0.045
R20	0.382	0.584	0.573	0.398
R21	0.655	0.123	*0.007	*0.019
R22	0.159	0.076	0.114	0.077
R23	0.060	*0.033	0.085	*0.001
R24	0.100	0.679	0.206	0.113
R25	0.100	0.456	0.308	0.102
R26	0.359	0.889	0.288	0.358
R27	0.100	0.987	0.871	0.362
R28	0.491	0.700	0.356	0.931
R29	0.096	0.840	0.700	0.113
R30	0.201	0.700	0.060	0.605
R31	0.077	0.097	0.109	*0.044
R32	0.947	0.910	0.342	1.000
R33	*0.002	0.366	*0.048	0.081
R34	*0.013	0.171	0.700	0.050
R35	0.400	0.200	0.700	0.297
R36	0.095	1.000	0.887	0.108
R37	*0.010	0.803	0.100	0.091
R38	*0.032	0.453	0.399	0.418
R39	0.100	*0.009	*0.023	0.050
R40	0.100	0.218	0.466	*0.012
R41	0.100	*0.030	0.058	*0.002

R42	0.202	*0.039	0.065	0.597
R43	0.179	0.114	0.100	*0.027
R44	*0.008	0.095	0.113	*0.011
R45	*0.003	0.948	*0.004	0.136
R46	*0.002	0.055	*0.012	*<0.000
R47	0.913	0.467	*0.006	0.570
R48	0.622	0.700	0.400	0.387
R49	0.768	0.111	0.107	*0.008
R50	0.378	0.502	0.083	0.387
R51	0.828	0.925	0.404	0.422
R52	0.093	*0.019	0.700	0.112
R53	0.665	0.100	0.906	0.436
R54	0.053	0.713	0.100	0.077
R55	0.420	0.174	0.295	0.962
R56	0.132	0.261	0.060	0.057
R57	*0.031	0.473	0.193	0.117
R58	0.212	0.482	0.553	0.497
R59	*0.047	0.278	0.400	*0.031
R60	0.530	0.100	0.292	0.656
R61	0.490	0.067	0.271	0.229
R62	*0.031	0.100	0.100	*<0.000
R63	0.400	0.283	0.644	0.666
R64	0.733	0.881	0.858	0.796
R65	0.088	0.868	0.779	0.588
R66	0.852	0.554	0.855	0.863
R67	0.400	0.188	0.564	0.127
R68	0.381	0.788	0.431	0.528
R69	0.658	0.700	0.400	0.791
R70	0.700	0.700	0.700	0.730
R71	0.852	0.763	0.100	0.231
R72	0.107	*0.009	0.129	0.258